FEBRUARY 1931

THESIS PRESENTED BY JAMES ORR, B.Sc.,

FOR THE PH.D. DEGREE

. Thesis. " Torsion in non-circular sections, considered analytically with experimental verification"

2. Paper to be published by the Aeronautical Research Committee. Confidential. (References to this paper by ')

3. Paper accepted by the Royal Society and in proof form. Confidential.

ProQuest LLC.
789 East Eisenhower Parkway
P.O. Box 1346
Ann Arbor, MI 48106 – 1346

The present research comprises --

(a) the development of an arithmetical trial and error method of finding the torsional rigidity of, and the stresses due to torsion in, bars with uniform non-circular section, and circular shafts with varying radius.
(Other methods were investigated and were found inferior to this one).

(b) tests on structural sections and on hollow square sections to find the torsional rigidity, the stresses, and the effective maximum stress which causes failure.

The present position of torsion research. The general differential equations for the torsion of bars with non-circular sections were obtained by St. Venant. These were solved by him for the ellipse, elliptical tube, equilateral triangle and rectangle. Solutions for many other simple forms of cross section have been obtained by the usual analytical methods -- a sector of a circle, a curvilinear rectangle bounded by two circular arcs and two radii, a hollow circular shaft with eccentric circular boundaries. As there are many cross sections of practical importance which can not be solved in this way, other methods have been developed for the general case of any chosen boundary.

Prandtl* called attention to the similarity of the torsion equations and the equations of equlibrium of a membrane stretched with uniform tension and subjected to pressure. This analogy was applied experimentally by Griffith and Taylor† using a soap film as membrane (see p. 4). They found the torsion

---

* Prandtl, Phys. Zeitschr., Bd.4 (1903).

† Griffith and Taylor, Aer.Res.Com., R & M, 333, 334, 392

properties of a number of sections, both solid and hollow, and from their results derived an approximate formula for solid sections (compared with my analytical and experimental results on p. 14'). / refers to the first accompanying paper.

Weber* developed simple formulae for structural sections by approximate analysis (compared with my results on p. 14').

Bairstow and Pippard† developed a method for the general case, evaluating a series of definite integrals graphically by means of a planimeter and special scales; this method is easily applied to most solid sections but is awkward for a serrated shaft with perhaps 30 serrations, since it necessitates using the complete section, and is very tedious in the case of hollow sections.

The general differential equations for the torsion of circular shafts of varying radius, were obtained by Michell‡. Solutions by the usual analysis have been obtained for a conical shaft, and one having the form of a paraboloid of revolution. The only method so far developed for the general case of any chosen boundary, is an approximate graphical one due to Willers‖.

Tests on bars with non-circular sections are not numerous. Bach¶ tested cast iron bars with rectangular, I , [, L sections, to destruction. He remarked on the weakness of the three latter sections in torsion and stated that the ultimate torque was about the same as that for a rectangular section of the same thickness and

---

* Weber, Forsch. H.249, V.d.I., 1921

† Bairstow and Pippard, P.I.C.E., 1921-22, II

‡ Michell, London Math.Soc.,31,1900

‖ Willers, Zeit.Math.Phys., Bd.55, 1907

¶ Bach, Elastizitat u. Festigkeit, 9th edn., pp.365-386

breadth equal to the sum of the web plus flange lengths. He made no analytical investigation. He also tested circular tubes with longitudinal slits, and his results show that St.Venant's equations do not apply to this case, since the end conditions cause normal stresses on the cross section (compare with my results for the torsion of the square tube with hole in one side, p.26').

Gibson and Ritchie* found the torsional rigidity of structural, and solid and hollow rectangular sections. They remarked on the small torsional rigidity of the I , [, and L sections, which they found to be $\frac{1}{100}$ to $\frac{1}{10}$ of the value obtained by assuming stress proportional to the distance from the axis of twist; they also remarked on the much greater torsional rigidity of box and hollow sections. They made no analytical investigation.

Campbell† found the torsional rigidity of a range of I beams and developed an empirical formula limited to this form of section. His experiments are specially interesting since he used strain gauges to find the stress on the flange face; he showed that the stress increases towards the centre of the flange face.

Moore‡ tested the weakening effect of keyways on the strength of steel shafts. He found the effect on the torsional rigidity and on the torque at the elastic limit. Gough‖ tested a pure iron and an 0.6% C steel shaft with keyway to the static elastic limit, and to fatigue failure under reversed stresses; he found also

---

* Gibson and Ritchie, The Circular Arc Bow Girder, 1914

† Campbell, Engin.News Record, 1928

‡ Moore, Univ. of Illinois, Bull.42, 1909

‖ Gough, Aer.Res.Com., R & M, 864, 1925

the torsional rigidity (see p.17').

Vedeler* found the torsional rigidity of rectangular tubes, built up from two channel shaped plates riveted together, fig.1. His results showed twists as much as double that given by the usual theory, whereas observation of the torsional vibration frequency of ships supports the usual theory, (compared with my experimental results on p.{25' / 18)

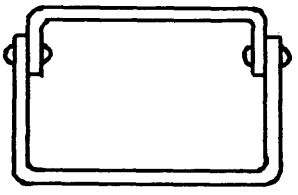

Fig.1.

The arithmetical trial and error method of solution is described fully in the two accompanying papers, pp.4' to 33' and 1" to 9" . Although the time to evaluate the torsional properties of any given section has been reduced to half-a dozen hours, this is out of all proportion to the time spent in the development of the method.

Experimental work done with the soap film method. The method is described fully in Aer.Res.Com., R & M 333. The following points are not discussed in these papers. In order to give the bubble a sufficient life for measurement purposes (5 to 15 minutes), fairly wet films had to be used. When the pressure is applied the film rises, commences to drain towards the boundary, at the junction of film and plate and causes a drop to gather. Fig.2 shows the section through a bubble with this sagging exaggerated. Now the stress at the boundary is given by the slope of the film there; as this can not be found owing to the sag, it is measured at

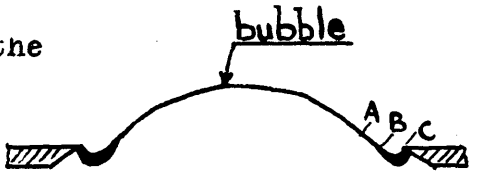

Fig. 2

---

* Vedeler, Trans.Inst.Nav.Arch., 1924.

A and B. The true slope at C is now estimated from these two readings.

Again, the method of obtaining the volume under the bubble by running a measured quantity of water out of a burette into the space below the bubble, was found useless. This was due to the initial sag, requiring an additional, unknown volume of water.

As a preliminary, the torsional properties of a shaft with square cross section were found by this method in order to gain experience and master the technique. A 2" square hole and a 2" circular hole were cut in the same plate. For the maximum stress in the square shaft, the maximum inclination of the soap film at the middle of one side was compared with the maximum inclination of the circular film. The following table gives the comparison.

Max.Incln. ⊙, α_1	Max.Incln. □, α_2	$\frac{\sin \alpha_2}{\sin \alpha_1}$	$\frac{\alpha_2}{\alpha_1}$
14°	18.7°	1.328	1.339
19°	26.0°	1.347	1.368
24°	32.5°	1.321	1.354
30°	40.9°	1.309	1.363

From the accurate solution, the ratio of the maximum stresses is 1.351, so, using the ratio of the inclinations of the films, gives this figure correctly to 1% for the range shown. Griffith and Taylor found the ratio of the sines to give the best results, but this difference in conclusion is probably due to their using drier films.

The torsional properties of a 2 × 2 × .375" B.S. T section were also found. Fig.3 shows the position of the holes on the plate; the T section is enlarged 2½

5, 2/10

FIG. 3.

2"×2" T ENLGD. 2½

Photographic Enlargement.

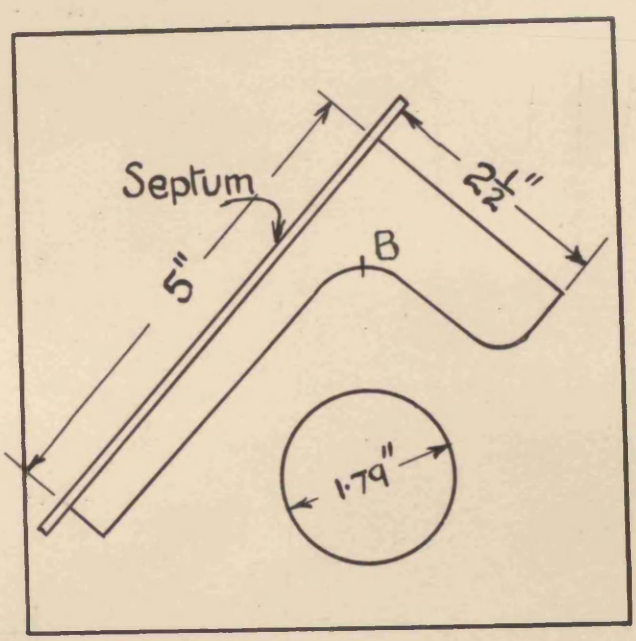

Position of Holes in Plate

Original Contours

times. In the case of a symmetrical section, such as the T, it is unnecessary to work with the complete boundary, for it has been found that the shape of a symmetrical film is unaltered if it be divided by a septum which passes through an axis of symmetry. It is therefore only necessary to cut half the section on the test plate. The diameter of the circular hole is obtained by making the ratio area/perimeter equal to that for the T. When this ratio is made equal in both films, the mean value of the sine of the inclination round the boundary of each film is also equal.

The maximum stress on the T section occurs at B, where the inclination is a maximum. A large number of observations were taken for this value for a wide range of inclination of the circular film, and the results are shown plotted in fig.4. With the exception of E and F, all the points were obtained from bubbles which had short life. These two points were obtained on a bubble which lasted three hours. The following table is based on the line through the points for the short life bubbles.

Max.Incln. ⊙, α_1	Max.Incln. T, α_2	$\frac{\sin \alpha_2}{\sin \alpha_1}$	$\frac{\alpha_2}{\alpha_1}$
15	23.5	1.540	1.57
20	31.7	1.537	1.58
25	40.3	1.531	1.61
30.5	50.0	1.510	1.64

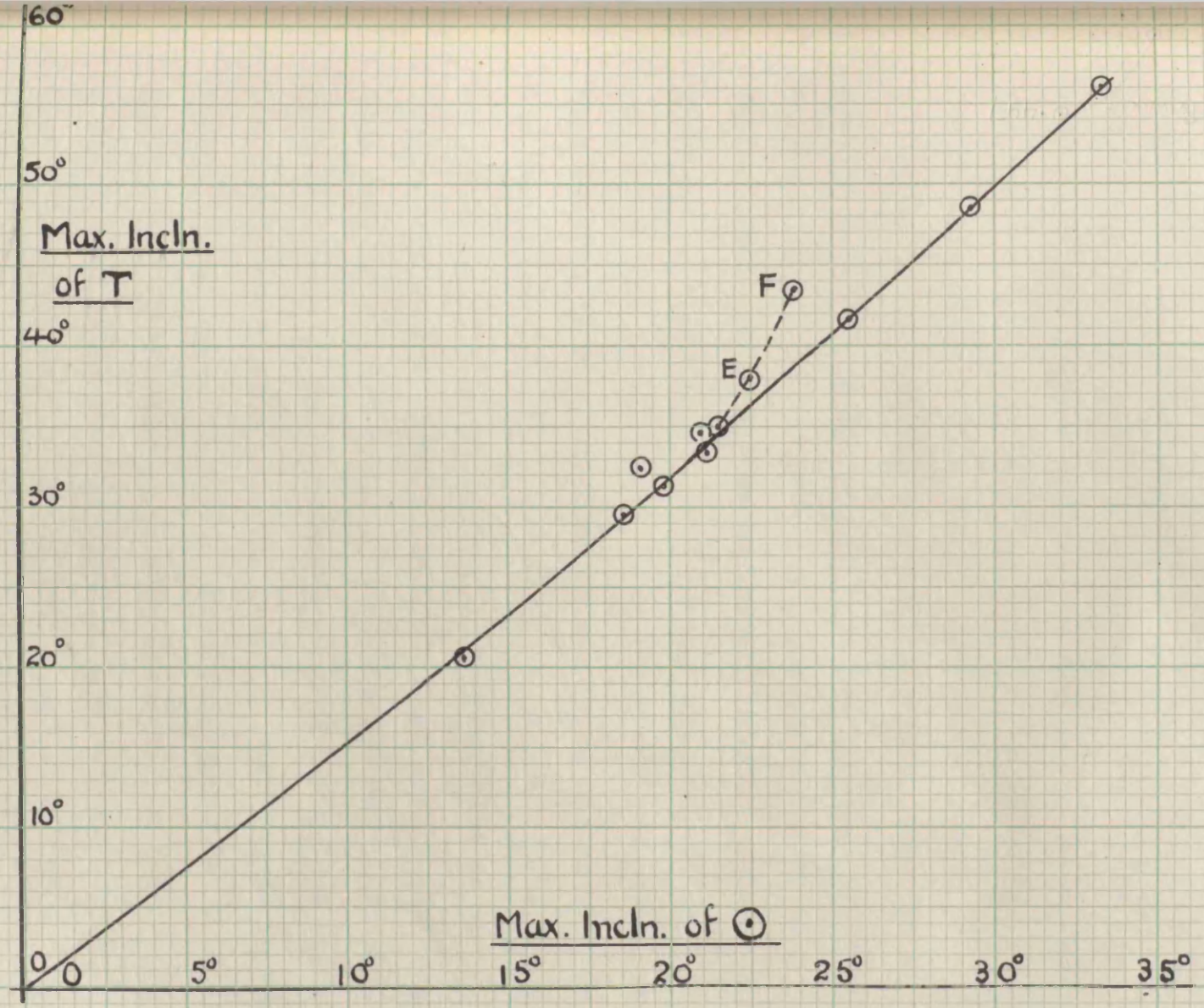
60°
50°
Max. Incln.
of T
40°
30°
20°
10°
0
F
E
0
5°
10°
15°
20°
25°
30°
35°
Max. Incln. of ⊙

FIG. 4

Taking the ratio of the maximum stresses as 1.57, we have for the T, Rmax = 1.57 × 0.895 = 1.40", since Rmax for the circle = the radius = 0.895" (for notation see p. 11'). Point F, fig.4, gives Rmax = 1.58". Griffith's approximate formula gives Rmax = 1.63", and this formula is up to 2% in error for structural sections (see p. 14'). So the short life bubbles give results much too low, while the long life bubble gives much better results. Since very few bubbles last more than ten minutes, we cannot depend on the results of soap film work for maximum stress.

Next, to find the torsional rigidity, contours were plotted. It was necessary to take the inclination of the circular bubble at frequent intervals of time since the bubbles varied with the varying temperature. The contours were obtained on black paper and a photographic enlargement was taken from this; fig.3 shows these for one experiment. Each contour is at a definite height above the plate; as the bubbles varied while taking the contours, these heights had to be reduced to correspond to a mean value of the inclination of the circular bubble. The area enclosed by each contour was now found by a planimeter and plotting this on a base of reduced height, enabled the volume under the bubble to be found. The ratio of this volume to the volume of the circular bubble corresponding to the mean inclination equals, approximately, the ratio of the rigidities. Thus we have finally, C = 2.80 in^4 . This result compares well with C_1 = 2.78 in^4 , from an approximate formula developed by the author (see p. 15').

In this research there was no further work done by this method, since its results for stress are doubtful, and the time and labour are greater than for the arithmetical trial and error method.

Tests on structural sections were carried out to find (a) the torsional rigidity, (b) the stresses, (c) the effective maximum stress causing failure. The test results for the torsional rigidity are summarised in the table on p. 14', and are there compared with the results of analysis and approximate formula. The effective maximum stress causing failure is discussed on pp. 20' to 22' There now follows a description of the experimental methods leading up to these results and some of the difficulties encountered.

The tests were carried out with a 100-ton Buckton machine, serving normally for tension and compression but having an additional arrangement for torsion. It is partly shown in the photographs and diagram, fig.5, where one may see the straining wheel, turned by hand through worm gearing, and the extension of the beam to provide a grip for the specimen. Although this arrangement has the advantage of accuracy in the measurement of the torque and rigidity in the end fixings, it has the disadvantage of shortness of gauge length and nearness of this length ~~of this length~~ to the grips. Hence special attention was given to end fixings and their effect on results. The length of specimen was 3', but the gauge length was limited to about 8" as shown in the diagram, fig.5. Possible error in the torque reading is negligible as the travelling load was $\frac{1}{8}$ ton and its position could be read by vernier to $\frac{1}{50}$". For a torque of 1 ton-in. the possible error is $\frac{1}{4}$% and all the beams were loaded beyond this value.

Twist was measured by two mirrors, attached to the specimen, and two telescopes which sighted on scales reflected in the mirrors. These are shown in the photographs, fig.5, and the mirrors are sketched separately.

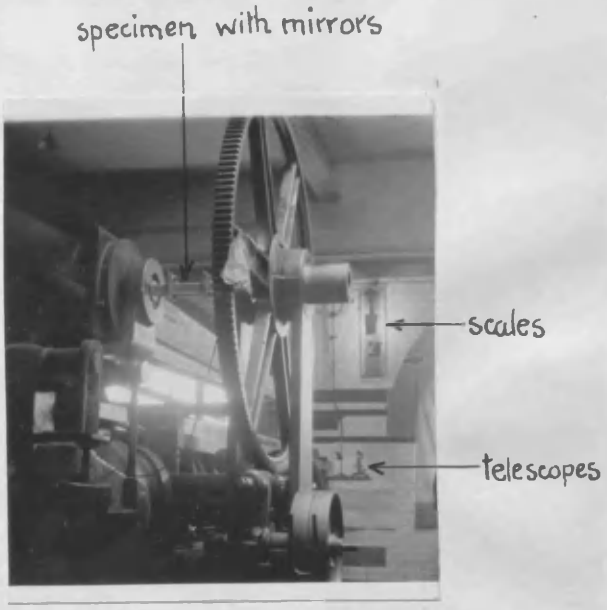

View showing telescopes.

View from telescope table

100^T Buckton Machine

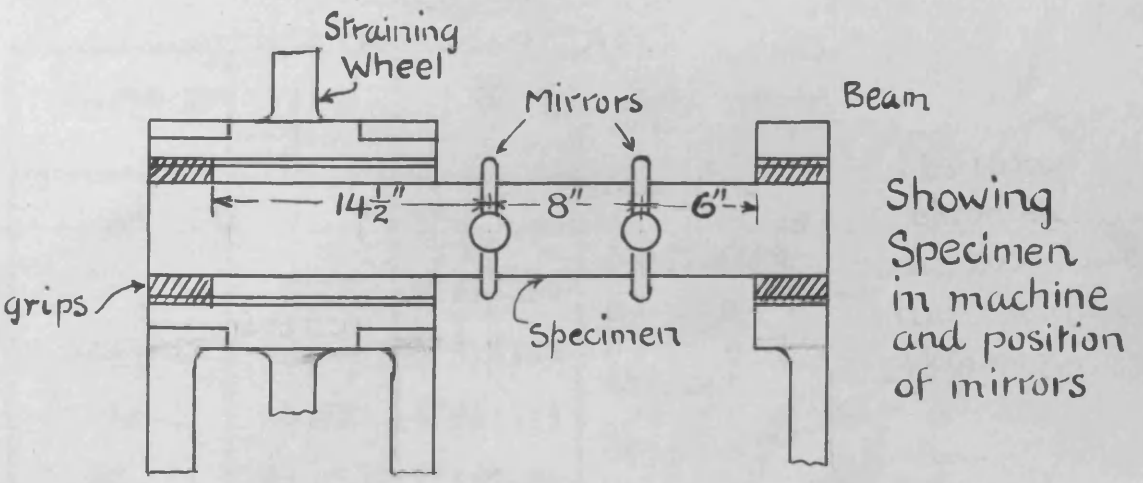

Showing Specimen in machine and position of mirrors

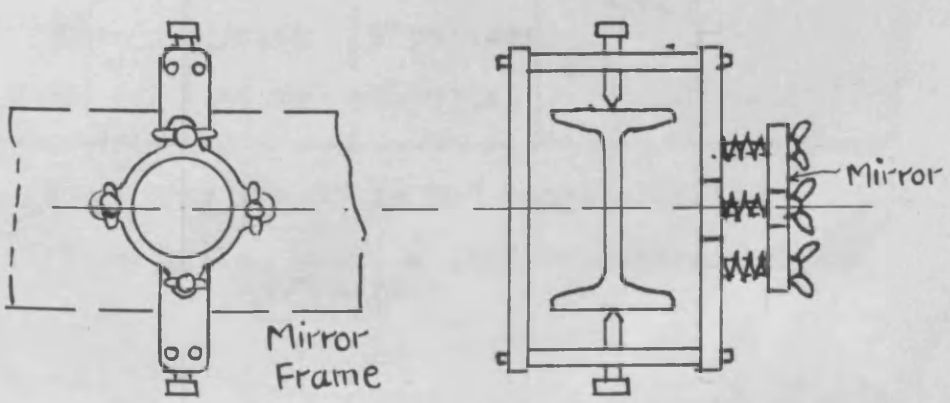

FIG. 5.

When the mirror rotates through an angle, the ray from the scale which coincides on reflection with the collimation line of the telescope, rotates through double the angle. This angle is approximately proportional to the scale reading difference. For great accuracy, a correction must be made for the tangent; it was found necessary to do this to obtain the limit of proportionality. The simplest method of correction is to add to the scale reading an increment to make it proportional to the angle. These increments are tabulated in the last column of the table, below. Fig.6 shows the relative positions of mirror and scale

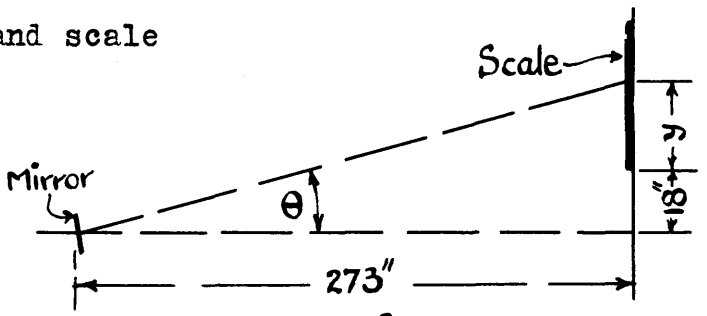

FIG. 6.

Height y	Scale Reading	θ	Δθ	Add to Scale Rdg
0"	0"	3° 46'.58		+0"
5	5.02	4° 49'.30	62'.72	+ .05"
10	10.04	5° 51'.83	62'.53	+ .08"
15	15.05	6° 54'.15	62'.32	+ .09"
20	20.06	7° 56'.20	62'.07	+ .09"
25	25.08	8° 57'.98	61'.77	+ .06"
30	30.10	9° 59'.40	61'.42	+0"
35	35.12	11° 0'.45	61'.03	- .09"

Mean over the 0" to 30" range = 62.14

1" on scale, mean, = .001800 radians of twist
(0" to 30")

As the scale may be read to 0.02" = 0.000036 radians, and as all the ~~beams~~ bars twisted by more than 0.018 radians on 8", before reaching the elastic limit, the error due to this factor is less than $\frac{1}{2}$%.

The design of the grips for holding the ends of the specimen and applying the torque, gave much trouble. First, a rigid grip was tried as shown in fig.7a. This consisted of keypieces fitting into the keyways in the beam and straining wheel, and transmitting the torque through $\frac{1}{2}$" diameter pins screwed into the specimen; cast iron blocks were also used to support the flanges. With these grips, the torque-twist curves ~~are~~ obtained are shown in fig.8a. They are looped instead of straight and the slopes are about 50% more than they should be. After consideration it was fairly clear that this was due to the rigidity of the grips imposing normal stresses on the cross section. This point is illustrated by the diagram, fig.7b. The centre line of the flanges, under pure twist, should take the form of a helix, ab. If the rigidity of the grip restrains it at the ends parallel to the axis, as shown at cd, the flanges take a transverse bending moment which causes normal stresses. Each flange acts like a beam, built in at both ends, one end deflecting relatively to the other. The case of a 6 x 3" I section is calculated numerically in fig.7b, where it is shown that the apparent torsional rigidity, when the stresses are purely normal, is fully double that for pure twist (we are neglecting in the first case the additional rigidity of the web). This would explain the high slopes of the curves, and also the looping, which ~~could~~ is due to variable restraint of the grips.

When the cast iron blocks were removed, the torque-

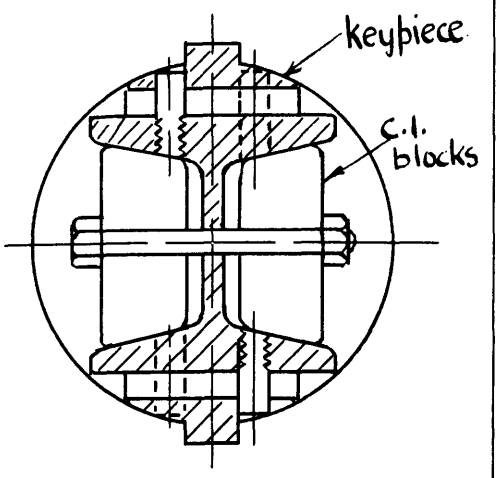

(a)

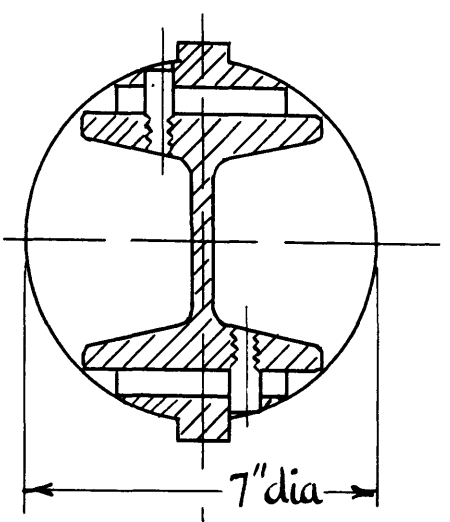

(c)

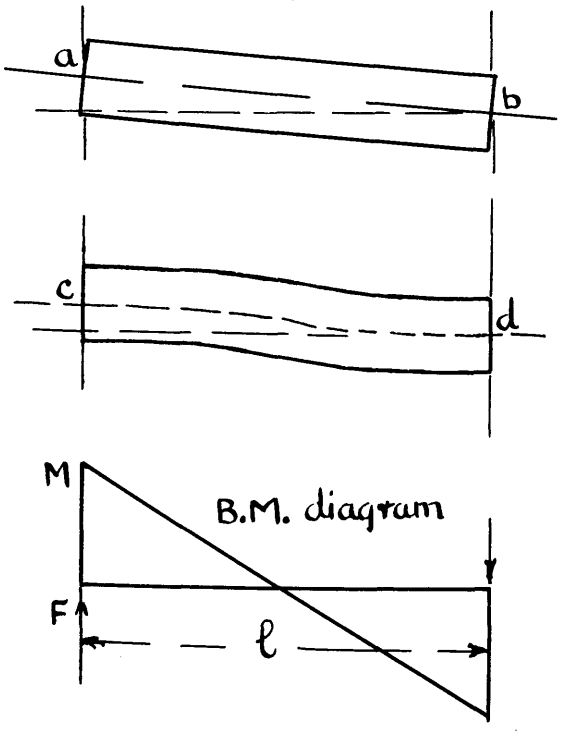

(b)

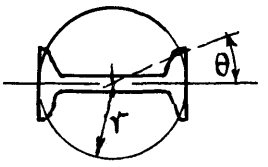

6"×3" I

With restraint as cd

torque due to bending = F×2r

$= \frac{12EIr\theta}{\ell^3} \cdot 2r$

$= 2544\frac{\theta}{\ell}$

E = 13,400 tons/in²

N = 5,300

r = 3", ℓ = 30"

I = $\frac{1}{12} \times 3^3 \times .35 = .79$

Slope at centre $= \frac{3}{2}\frac{r\theta}{\ell}$

$\frac{T}{T_{bending}} = 1700$

With pure twist

$\frac{T}{T_0} = 809$

EFFECT OF DIFFERENT GRIPS

FIG 7

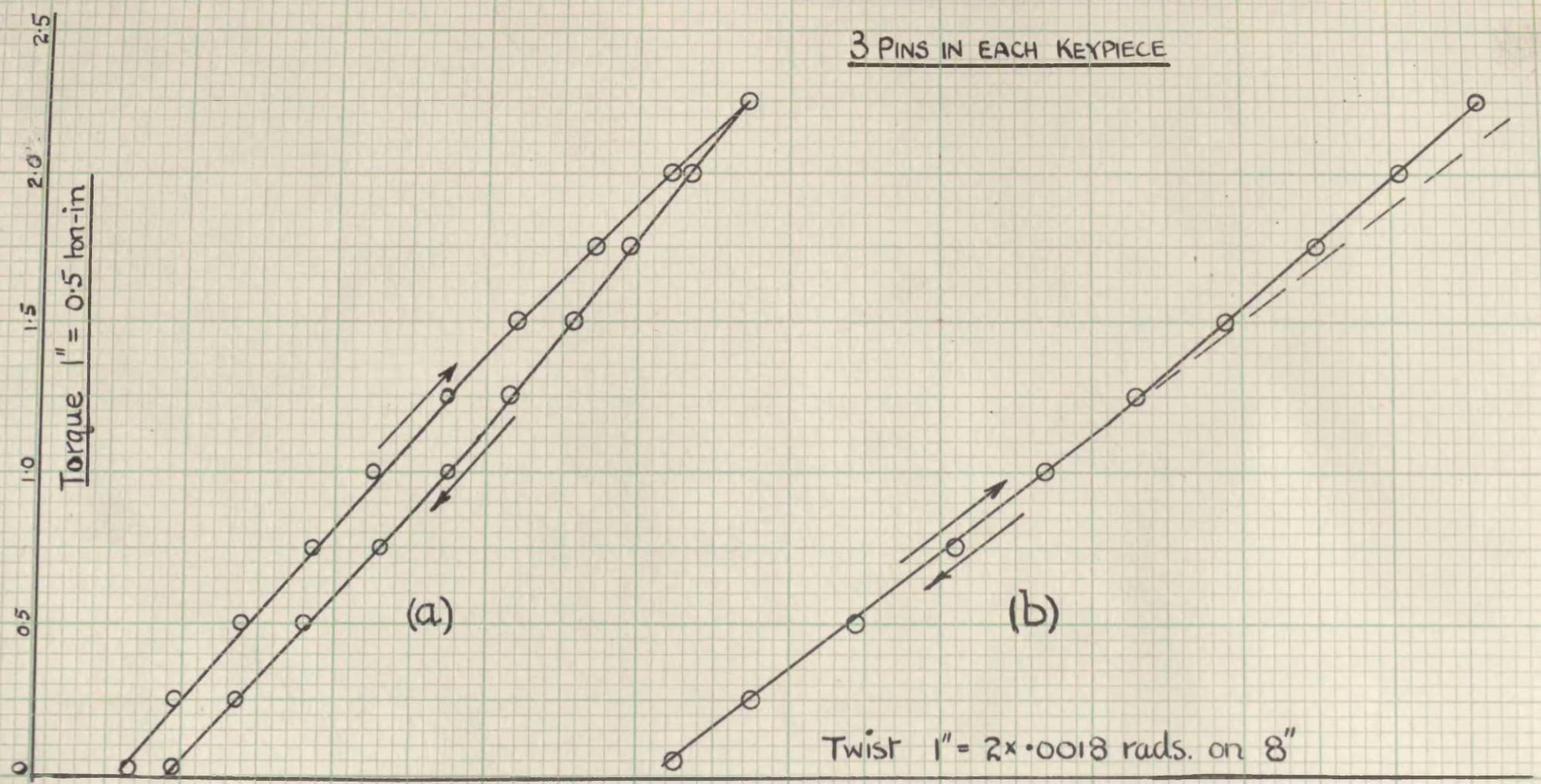
CURVES FOR 6"×3" I BAR WITH
3 PINS IN EACH KEYPIECE
Torque 1" = 0·5 ton-in
0
0·5
1·0
1·5
2·0
2·5
(a)
(b)
Twist 1" = 2×·0018 rads. on 8"

FIG. 8

twist curve had no loop, but became steeper at the higher loads, fig.8b. Thus less restraint in the grips improved the curves. Finally, by taking away two of the three pins in each keypiece, as shown in fig.7c, and using grease to eliminate friction, the curves became straight lines (see later).

Next, the effect of proximity of the grip to the gauge length was investigated. This was done by two methods; firstly, by means of tensometers the actual stresses were found throughout the gauge length and secondly, by moving one mirror 3" nearer the grip, the twist was found for the new gauge length and compared with the twist for the old. Both methods showed that the gauge length was quite clear of end effects. ~~The details of these tests are given later, p.~~ .

Torque-twist curves were now obtained after the preliminary investigation, for the following sections -- $5 \times 4\frac{1}{2}$" I, 6×3" I, 4×3" I, 6×3" [, 2×2" L. The procedure was to estimate a safe range of torque for a section, and load it through this range twice, taking readings of twist. When straight lines were obtained, coincident for loading and unloading, the load was increased above this range by small increments until the bar had taken a considerable permanent set. Figs.9 and 10 show the curves for these sections. From the straight line part of the curves, the torsional rigidity of the sections is found; it is given in column 3 of the table on p. .

Our next consideration is the failure of the bar. Firstly, the limit of proportionality is a possible criterion. To obtain this, the curves are replotted, the abscissa now giving the divergence of the twist from

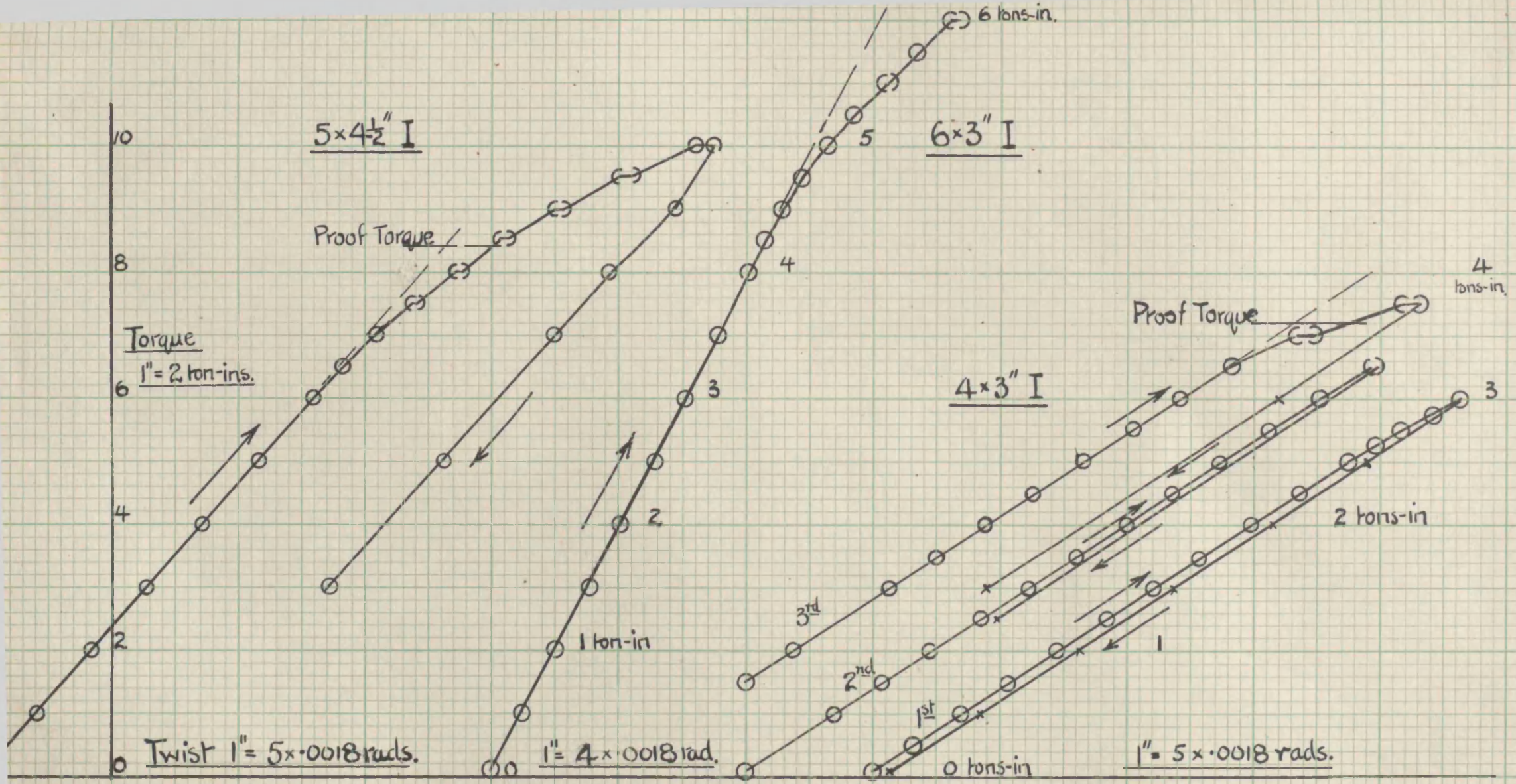
5×4½" I
6×3" I
4×3" I
Proof Torque
Torque
1" = 2 ton-ins.
Twist 1" = 5×·0018 rads.
1" = 4×·0018 rad.
1" = 5×·0018 rads.
1 ton-in
2
3
4
5
6 tons-in.
4 tons-in.
2 tons-in
0 tons-in
1st
2nd
3rd
0
2
4
6
8
10

FIG. 9.

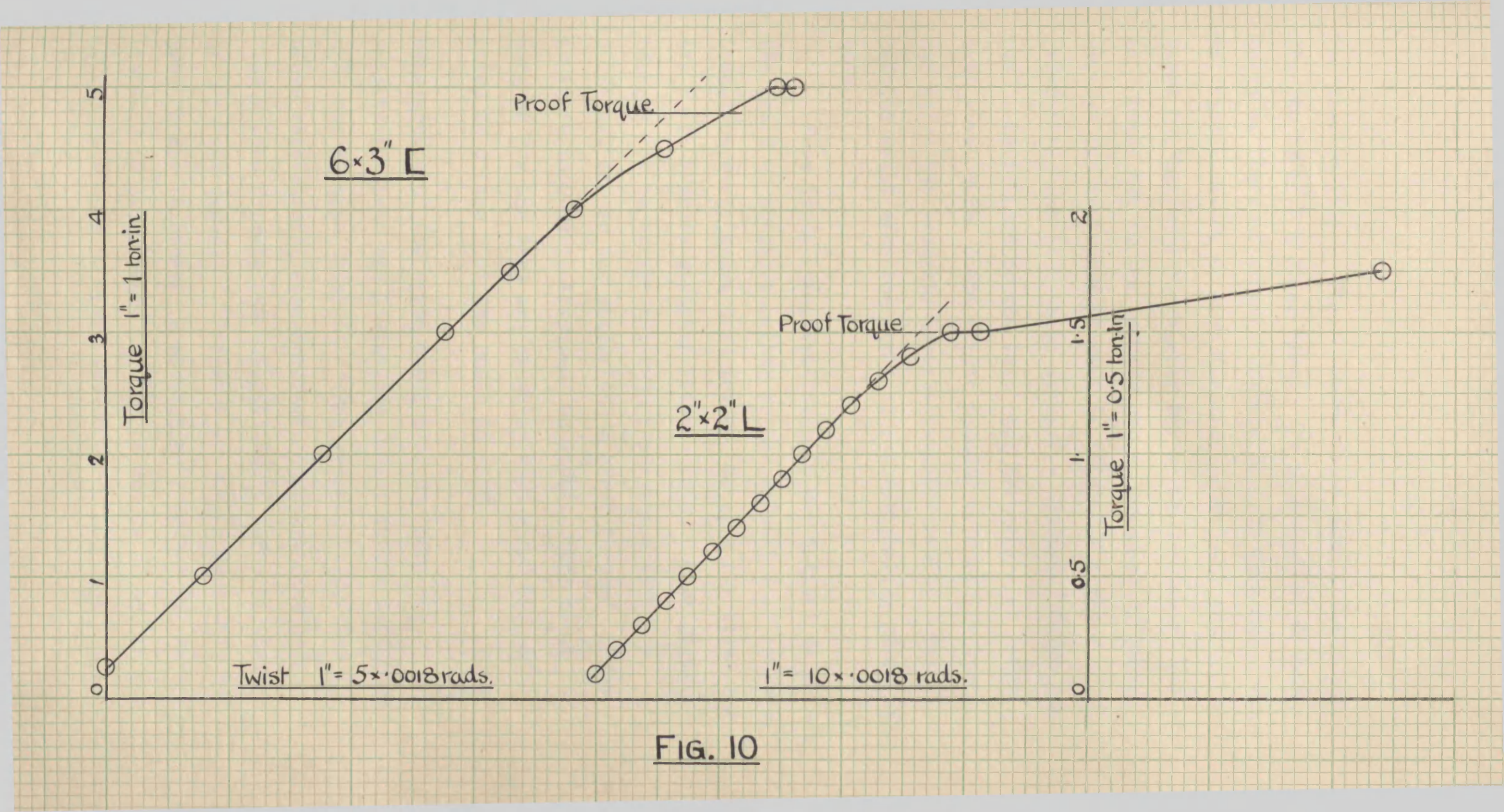
6×3" L
Proof Torque
Torque 1" = 1 ton-in
0
1
2
3
4
5
Twist 1" = 5×·0018 rads.
2"×2" L
Proof Torque
Torque 1" = 0·5 ton-in
0
0·5
1·
1·5
2
1" = 10×·0018 rads.

FIG. 10

the elastic line. Fig.11 shows these curves for F1 and F2, two 5 × 4½" I section bars. It is seen that F1 has a definite limit of proportionality at 6.25 tons-ins., but F2, test A, shows no such definite point, and, test B, shows the improved elasticity due to the permanent set of A. These two latter tests show the weakness of taking this as the criterion of failure, for in A it is indefinite, and in B it is altered. Further, Guest and Lea*, investigating the torsional hysteresis of round mild steel bars, found slight looping at very low loads, far below the commonly accepted elastic limit. Their results would make the limit of proportionality practically zero.

From these considerations, it was decided to abandon the limit of proportionality as the criterion of failure. Also, the yield point will not do, as only the curve for the 2 × 2" L shows anything like a yield. Thus we are finally led to choose a torque producing a definite permanent set as the criterion, a proof torque. This point is more fully discussed on p. 20'. The proof torques for the bars are shown in figs.9 and 10, and given in column 5 of the table on p. 22'.

Measurement of the cross section of the bars was undertaken since the dimensions were a little different from the British Standard. The aim was to measure the cross section with such accuracy, that analysis or approximate formula (if correct) would agree to within 1% of the test figures. Consider a 5 × 4½" I section; the mean flange thickness is about 0.45", and as the torsional rigidity is proportional to the thickness cubed, this measurement must be made correct to 0.0015" for 1%

*Guest and Lea, Proc.Roy.Soc., A93, 1916.

Search for Limit of Proportionality in Two 5×4½" I Bars.

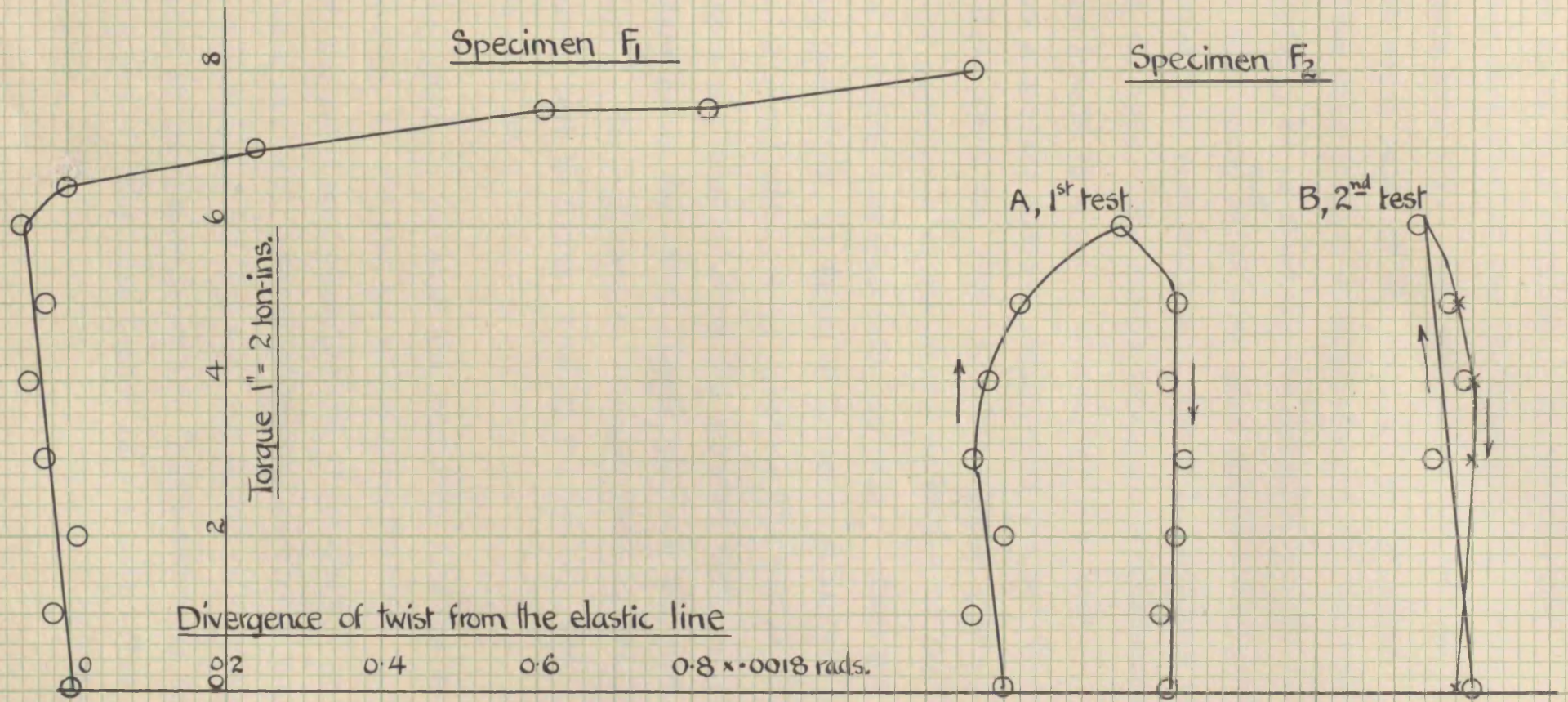

Fig. 11.

accuracy. This was almost impossible considering the rolled surface and the irregularities, yet an attempt was made to work up to this standard. By having three specimens for each size of bar and measuring all these, helped towards this aim. The surface of the bar was cleaned with emery paper at the ends and in the gauge length. Even this cleaned surface was not the same as a machined surface, as is shown by the results for the rectangular specimens, p.15 which also show the amount, 0.001", to be deducted from each surface. The web thickness was measured at the ends. The flange thickness was measured in the gauge length by a point micrometer with base suitable for a surface table. Supporting the bar at a definite height above the table with the flange face vertical, the micrometer measured the thickness of the flange at a definite distance from its edge. This was done for two positions, as shown at A and B in fig.12, which is an original obtained by upending the bar on the table on paper and drawing round the contour with a sharp pencil. This gives the other dimensions, and the root and toe radii. The approximate formulae were applied to these measured test sections, finding C1, C2, C3, and Rmax, shown on p. 14'.

Tests on Specimens. To find the rigidity modulus, N, Young's modulus, E, and the stress causing failure, for the material of the sections, circular and rectangular specimens were cut out. The rectangular specimens were taken from the flanges and web and the circular from the thick portion at the junction of the flange and web, as shown in fig.20'. They were tested in a single lever torsion machine, which is sketched in fig.13. As there

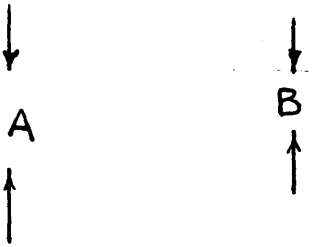

FIG. 12

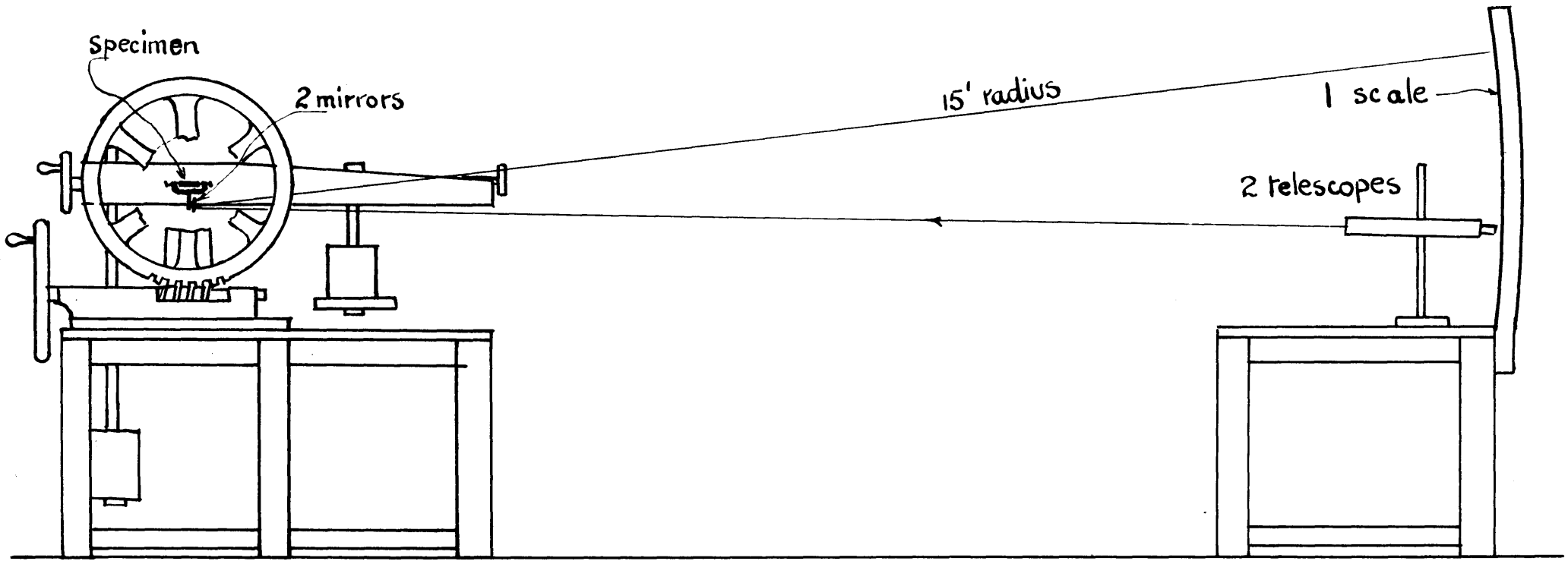

FIG. 13.

was no suitable twist measuring apparatus, one had to be schemed out. The arrangement was similar to that on the previous (100 ton Buckton) machine. A curved scale was used, fig.13, to avoid correcting for the tangent, and it was placed 180" distant from the specimen.

The frames for the mirrors are shown in full in fig.14. Parts (1) and (2) are made of cast aluminium, part (3), which holds the mirror, of strip brass, and part (4) of brass rod. The rotation which is important, is that round the axis YY, so this is controlled by screw A and spring B and these give also the zero adjustment. The rotations round the other two axes are not important, since a movement there would not affect the scale reading. A friction control is therefore sufficient and this is aided in the case of rotation round XX by suspending the frame from the specimen.

The grips used for the rectangular and circular specimens are sketched in fig.15. It will be noted that failure will occur first in the grips of the circular specimens, but this will not affect the results since this is a local effect. This figure also shows the position of the mirrors on the specimen.

Torque-twist curves for the specimens from F2, a $5 \times 4\frac{1}{2}$" I bar, are shown in fig.16. The slope of the elastic line gives the ratio $T/\tau = N \times C$. C may be found easily in the case of the circle, and from tabular values in the case of the rectangule (calculated by St. Venant) and hence N may be found from these curves. The values obtained in this way are given in the following table.

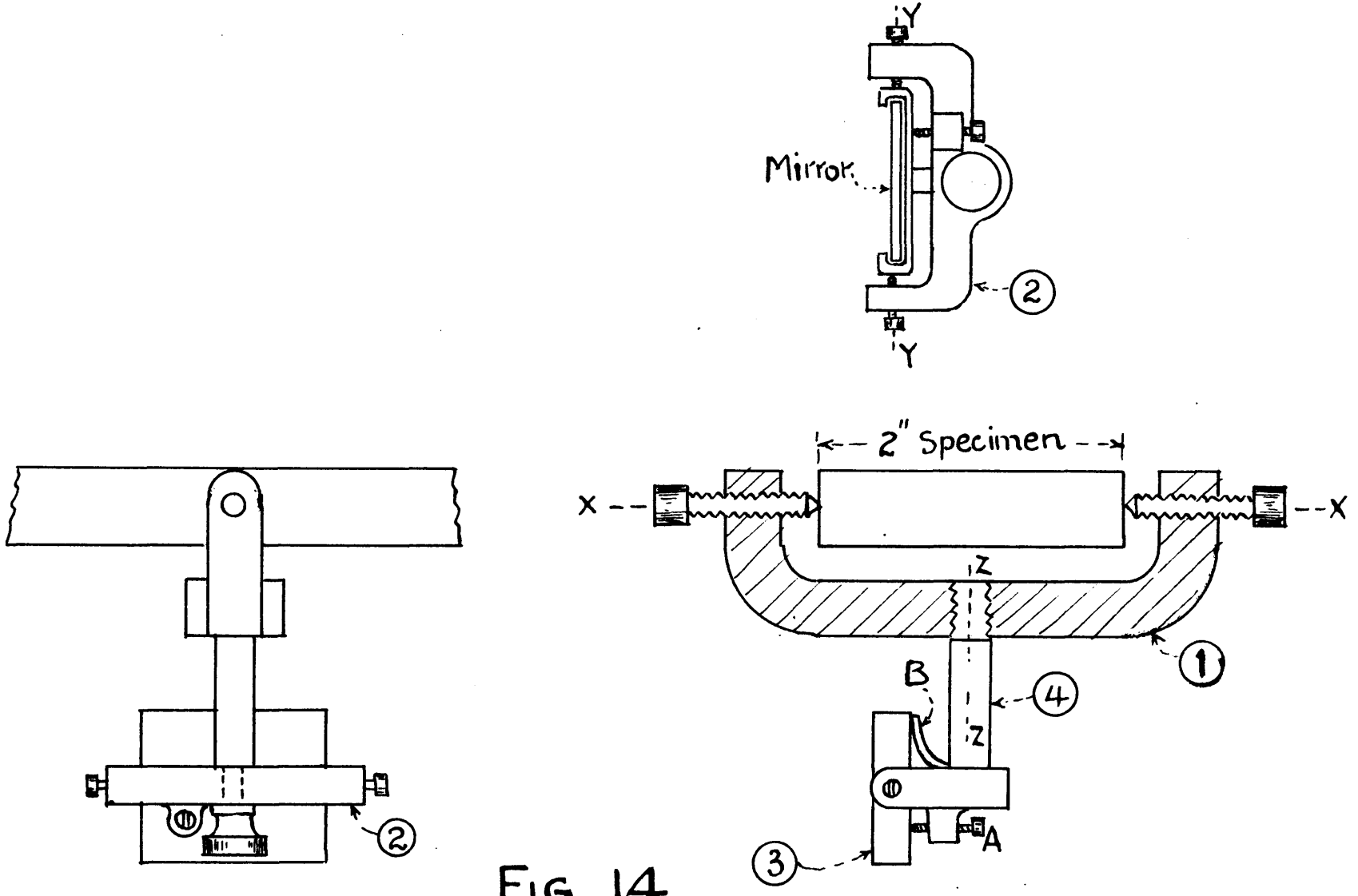

FIG. 14.

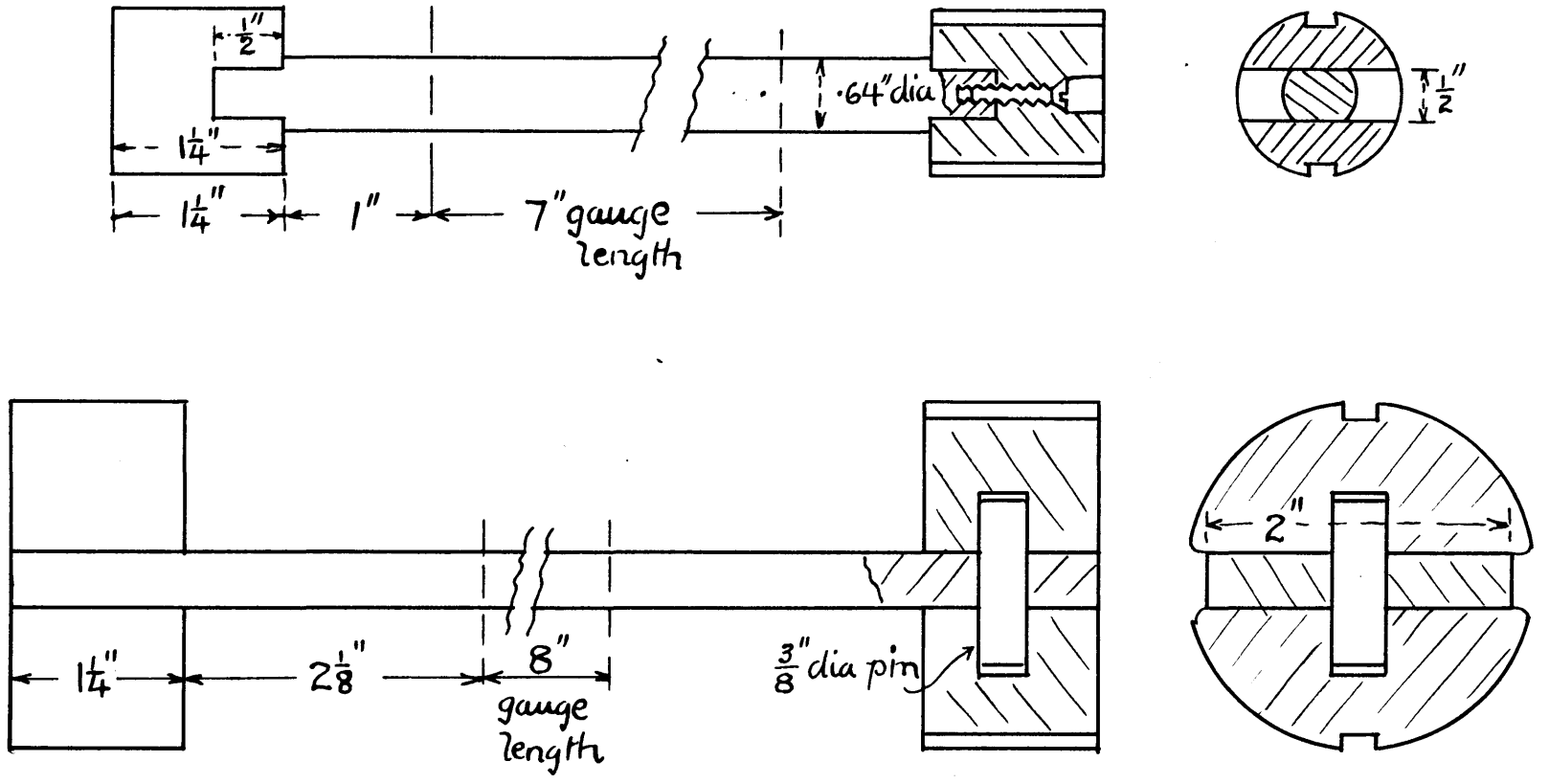
1/2"
1 1/4"
.64" dia
1/2"
1 1/4"
1"
7" gauge length
1 1/4"
2 1/8"
8" gauge length
3/8" dia pin
2"

FIG. 15

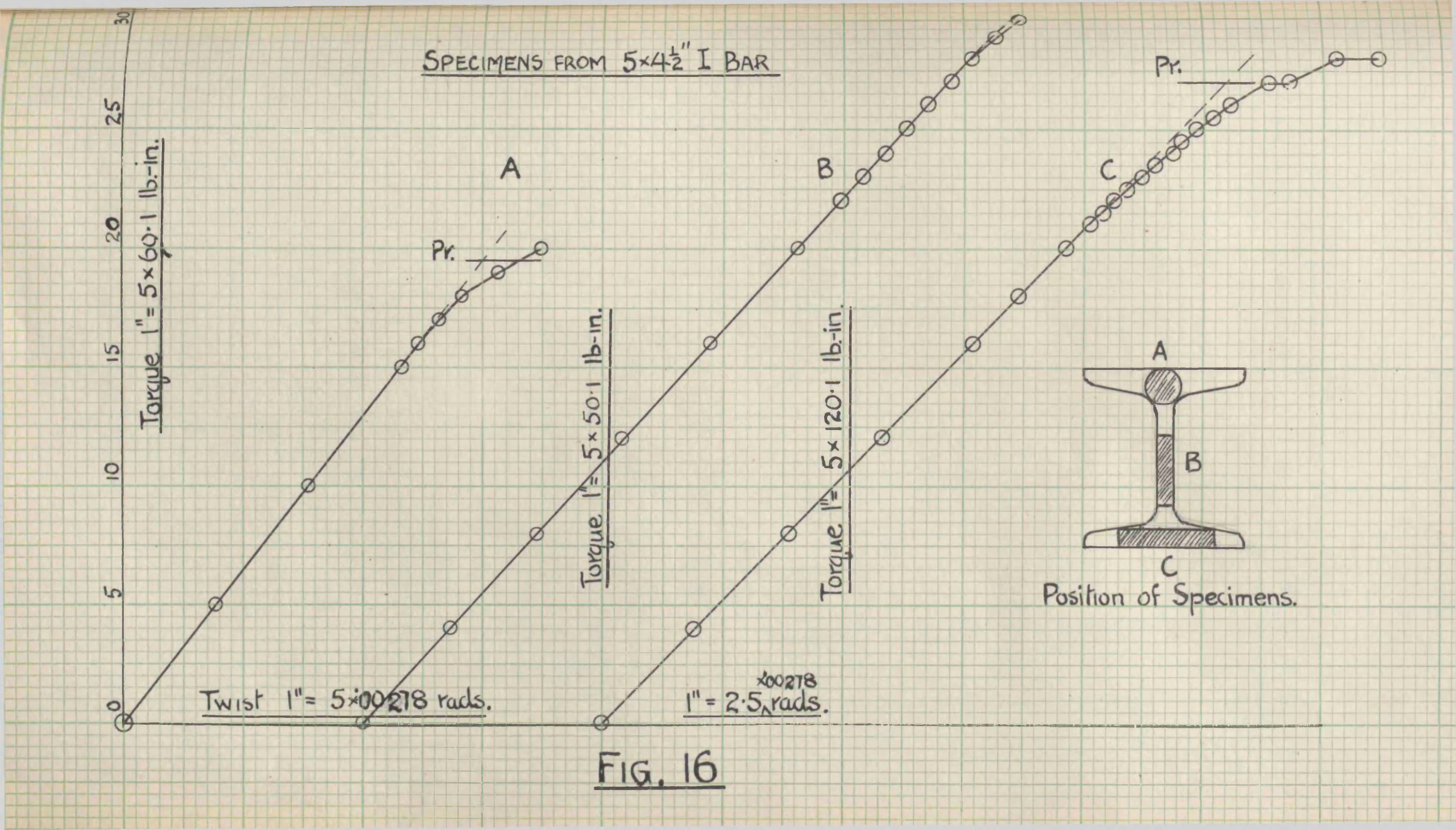
SPECIMENS FROM 5×4½" I BAR
A
B
C
Pr.
Pr.
Pr.
Torque 1" = 5×60·1 lb.-in.
Torque 1" = 5×50·1 lb.-in.
Torque 1" = 5×120·1 lb.-in.
Twist 1" = 5×·00278 rads.
1" = 2·5×·00278 rads.
0
5
10
15
20
25
30
A
B
C
Position of Specimens.

FIG. 16

Specimen	Dimensions	C	N lb/in^2
6 3" I			
web rough	2.024 × 0.2817"	0.01371 in.^{4}	(11.42)10^6
web smooth	2.024 × 0.2757	0.01289	11.68
flange	2.012 × 0.2883	0.01456	11.70
circle	0.5005 diam.	0.006160	11.79
5 4½" I			
web rough	2.010 × 0.2895	0.01473	(11.57)
web smooth	2.010 × 0.2819	0.01364	11.70
flange	2.025 × 0.4753	0.06198	11.63
circle	0.6429 diam.	0.01677	11.68
6 3"			
web	2.02 × 0.257	0.01043	11.70
flange	2.01 × {0.425 / 0.344}	0.0400	11.60

The results for web specimens with unaltered surfaces give low values of N. On cleaning the surfaces and retesting, N is raised to consistency with the other results. Rough surfaces evidently cause measurements to be too great. By deducting .001" from each rough surface, and considering this as the true thickness, would raise N from 11.42 to 11.68. This amount was also deducted from the measured thicknesses of the structural sections.

From these curves, fig.16, may be found also the maximum shear stress at failure (at the proof torque). The torque and maximum stresses are tabulated on p.22'.

It is necessary to know Poisson's ratio for the material in order to find shear stress from tensometer strain readings. This was done in two ways; firstly,

a rectangular specimen was pulled in a testing machine. The longitudinal and transverse strains were found with tensometers, and the ratio of these is the required result. Secondly, Young's modulus may be found from the same test by finding the stress. σ may then be calculated from

$$E = 2N (1 + \sigma)$$

A flange specimen from a 6 × 3" I bar gave the following - $N = 11.7 \times 10^6$ lb/in^2. First method $\sigma = 0.30$. Second method, $E = 30.5 \times 10^6$, $\sigma = 0.30$.

The breaking stress in tension was also obtained, to give a basis when considering maximum shear stresses. This figure varied from 29.4 to 32.2 tons/in^2.

Tests on hollow square tubes. The test results are discussed on pp. 24' - 26'. The specimens were solid drawn circular tubes, hammered to square form, $3\frac{1}{4}" \times 3\frac{1}{4}"$ outside dimensions. There were three specimens, thicknesses .171", .173", and .233". They were carefully annealed by heating to 850° C during 1 hour, and cooling slowly in the furnace during 18 hours. It was hoped by this method to eliminate as far as possible the stresses caused by the hammering, although initial stresses were not expected to affect appreciably elastic results, ~~which was~~ and these were the chief aim of this experiment.

These tubes were tested in the 100 ton Buckton machine. The length of the tubes was less than that of the structural specimens, being 25", yet this still allowed a gauge length of 8" and a distance of 7" between mirror and grip.

The grips again gave trouble. First there was tried the arrangement, which was successful in the case of structural sections, fig.7c. Here, large loops were

obtained, as shown, fig.17a, and the twists were considerably greater than indicated by analysis (3 or 4 times). Fig.18a shows the arrangement used here with one pin in each keypiece. When loaded, the cross section takes the form at the ends as shown exaggerated in fig.18b. If the tube were very long, probably St. Venant's principle that the strains which are produced in an elastic solid, by the application to a small portion of its surface of a system of forces statically equivalent to zero force and zero couple, are of negligible dimensions at distances which are large compared with the linear dimensions of that portion, would apply. If this were so, the centre portion would behave in agreement with analysis. It is therefore concluded that the shortness of the specimen does not permit the neglect of end conditions, which causing stresses so far removed from the required distribution. The aim, then, is to distribute the stresses at the ends more favourably. This was done by making the grips much more rigid, as shown in fig. 17', when the graph became straight, fig.17b.

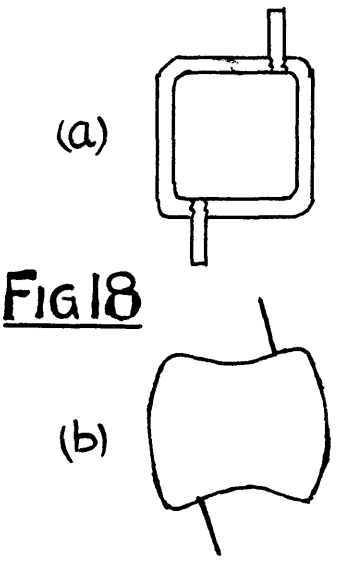

FIG 18

Evidently the question of grips is very important in torsion testing of non-circular sections, especially if the specimens are short. This conclusion may be applied to actual cases in practice, and there a careful investigation of end conditions would be required before attempting to find stresses.

From the curves, the torsional rigidities of the sections are found. It should be noted that the twists

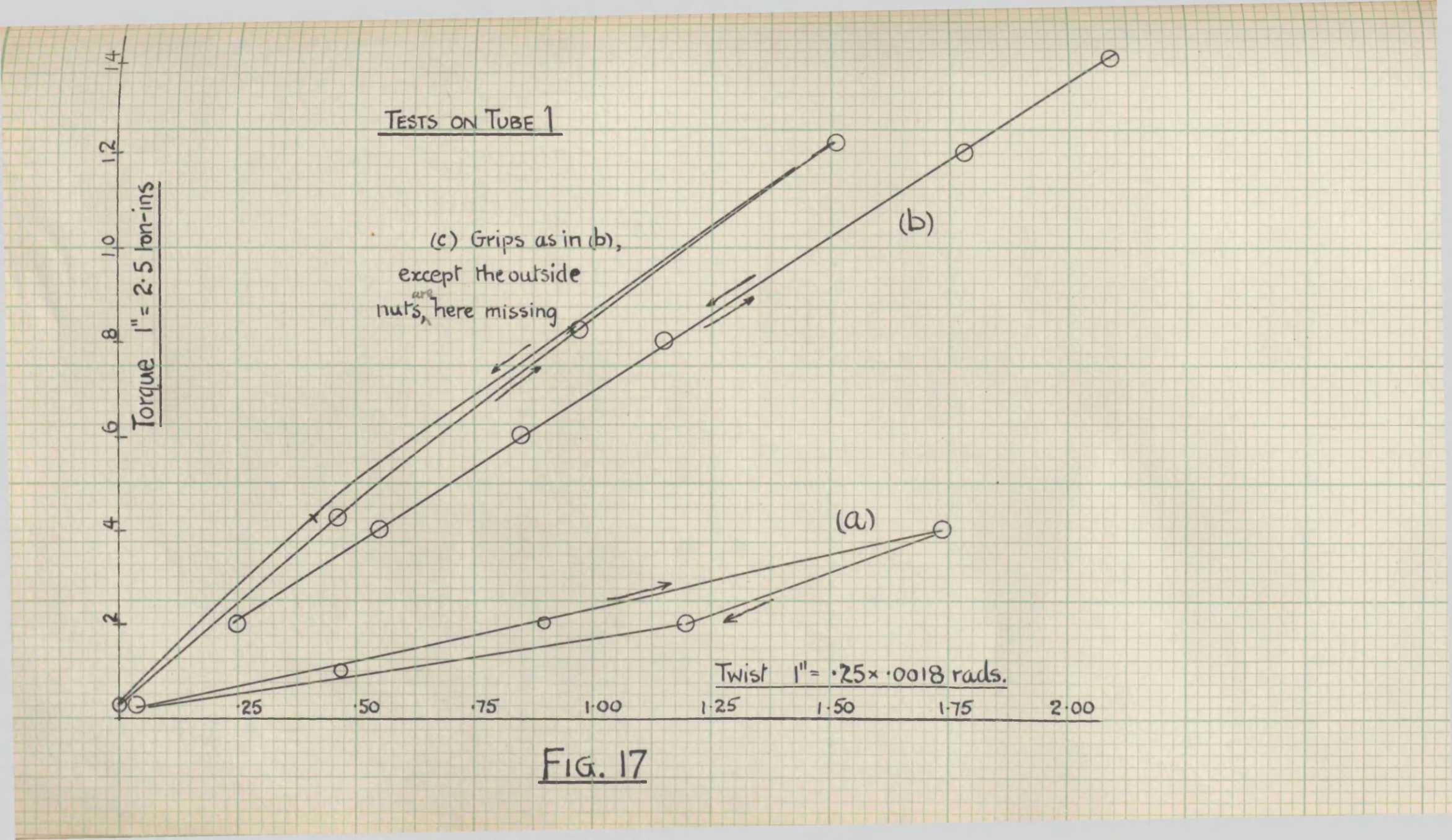
TESTS ON TUBE 1
Torque 1" = 2·5 ton-ins
·2
·4
·6
·8
1·0
1·2
1·4
(c) Grips as in (b), except the outside nuts are here missing
(b)
(a)
Twist 1" = ·25 × ·0018 rads.
·25
·50
·75
1·00
1·25
1·50
1·75
2·00

FIG. 17

are small, about 2" difference on the scales. Since the scale can be read to 0.02" and there are two subtractions to obtain a twist, the maximum reading is possibly 4% in error. Drawing a line through a number of values will reduce this somewhat, to perhaps 2%

The following table gives the results.

Torsional Rigidity of $3\frac{1}{4}$ $3\frac{1}{4}$" Square Tubes, C

Tube	Expt.	Approx. C' Formula	2nd C" Approx.
1 (.171")	5.6 in.	5.28 in	5.40 in
2 (.173)	5.36	5.08	5.20
3 (.233)	7.20	6.83	7.10

In this table the approximate formula, which assumes stress constant across the thickness is

$$C' = 4A^2 t / P$$

where A is the mean of the areas enclosed by the inner and outer boundaries, P is the mean length of the inner and outer boundaries and t is the thickness.

From the results of analysis on the hollow square (see p.25'), the second approximation is derived

$$C'' = 2B (a^2 - 1.92at + 1.92t^2)$$

where $B = a^2 t / (2a - 2.48t) - t^2$, and a is the outside dimension of the square.

There is really good agreement between theory and experiment, compared with the large discrepancies due to end conditions.

The stresses were found by tensometers, using 1" gauge length. To find the complete system of stress on

a surface by this method, the strains along three directions are required, e1, e2, e3. When pure shear is acting on planes at right angles to the surface along the directions e1 and e2, then e1 =-e2, and e3 = 0. These three strains were measured at the centre of the flange faces and at a point $\frac{3}{4}$" from the edge. The following table gives typical results for tube 2. These figures were obtained by the following procedure -- start at 1 ton-in., take readings, run load to 6 ton-in., then to 11, then back to 6 ton-in., at each load position taking readings of the tensometers. If they were not consistent, the clamping of the tensometer was suspected.

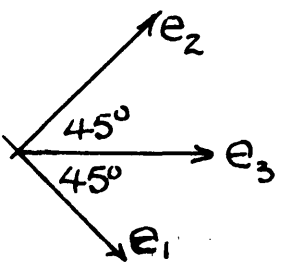

Strain $\times 10^4$ for Torque = 10 ton-in.

Dirn.	Top Centre	Under Centre	Front Centre	Back Centre	Front Edge	Back Edge
e1	3.58	3.67	3.00	3.69	3.50	3.36
-e2	3.04	3.20	4.17	3.45	3.21	3.52
e3			-.17	0	-.08	0

Mean value of e = 3.43×10^{-4}

Shear stress, $q = Ee / (1 + \sigma)$

$= 3.43 \times 10^{-4}\ 1.34 \times 10^{4} / 1.29$

$= 3.56$ ton/in^2.

From the approximate formula, $q = T / 2At$, assuming the stress constant over the cross section. This equals here $q = 3.08$ ton/in^2. Allowing for the increase of stress from inside to outside, this figure would be raised to $q = 3.25$ ton/in^2. The other two tubes gave similar results.

CONFIDENTIAL.

T.3003.
(Strut.9).

T.3003.
(Strut.9).

AERONAUTICAL RESEARCH COMMITTEE.

Several cases of non-circular torsion solved by analysis and direct test.

- By -

James Orr, B.Sc.

Presented by Professor J. D. Cormack.

September, 1930.

1. Introduction.

1.1. Purpose.- The purpose of the paper is to demonstrate an arithmetical trial and error process, solving the torsion problem for any chosen boundaries. By its use several British Standard structural sections, a shaft with keyway, a hollow square, a hollow serrated shaft, a circular shaft enlarging to greater diameter, and a shaft with a collar have been solved. These results are checked by tests in the case of the structural sections and hollow square by measuring both the twist and stresses. Also, the failure of a prism subjected to local high stresses is discussed.

1.2. Equations.- When a prism is subjected to terminal couples about its axis (Oz), the stresses and strains are found by solving the equation*

$$\partial^2\psi/$$

* Love's Mathematical Theory of Elasticity, 4th. ed. Ch.14.

$$\frac{\partial^2 \Psi}{\partial x^2} + \frac{\partial^2 \Psi}{\partial y^2} + 2 = 0 \quad \ldots\ldots (1)$$

throughout the cross-section (x0y), keeping Ψ constant on each boundary. The shear stress components are given by

$$X_z = N\tau \cdot \frac{\partial \Psi}{\partial y}, \quad Y_z = N\tau \cdot \frac{\partial \Psi}{\partial x}$$

where N is the modulus of rigidity of the material and τ is the twist per unit length of the prism. The maximum stress occurs on a boundary, and is given by

$$q_{max.} = N\tau \cdot \frac{\partial \Psi}{\partial n} = N\tau \sqrt{\left(\frac{\partial \Psi}{\partial x}\right)^2 + \left(\frac{\partial \Psi}{\partial y}\right)^2}$$

where ∂n is the element of the normal to the boundary. The torque T is equal to $T = 2N\tau \cdot \iint \Psi . dx . dy$ in the case of solid sections.

The equation for a circular shaft of varying diameter subjected to terminal couples about its axis (0z), is*

$$\frac{\partial^2 \psi}{\partial r^2} - \frac{3}{r} \cdot \frac{\partial \psi}{\partial r} + \frac{\partial^2 \psi}{\partial z^2} = 0 \quad \ldots\ldots (2)$$

where ψ is constant on the boundary, using cylindrical co-ordinates $r\theta z$. The stress components are

$$\hat{\theta z} = \frac{N}{r^2} \cdot \frac{\partial \psi}{\partial r}, \quad \hat{r\theta} = -\frac{N}{r^2} \cdot \frac{\partial \psi}{\partial z}$$

1.3/

---

* Love's Mathematical Theory of Elasticity, 4th. ed. Ch.14.

1.3 Other methods.- These equations have been solved by the usual analytical methods only for certain boundaries. Thus (1) has been solved for the ellipse, the elliptical tube, the rectangle, a sector of a circle, a circular tube whose inner and outer boundaries are not concentric, (2) for a conical shaft and a paraboloid of revolution.

Several methods have been discovered of solving the problems for any chosen boundary.

Bairstow* and Pippard have developed a method for solving (1), evaluating a series of definite integrals graphically by means of a planimeter and special scales; this method is easily applied to most solid sections but is awkward for a serrated shaft with perhaps 30 serrations, since it necessitates using the complete section, and is very tedious in the case of hollow sections.

Taylor+ and Griffith used an approximate analogy to solve (1), experimentally by means of soap films; once the apparatus is gathered and the technique mastered this method gives quick results, but the accuracy is doubtful in some cases, and this is illustrated by an experiment on a T section. In this experiment, the maximum stress at

the/

---

* Bairstow and Pippard, P.I.C.E. 1921-22, II.

+ Taylor and Griffith, Aero. Res. Comm., R.& M.s. 333 and 392.

the junction as measured by the ratio of the inclination of the film to that of the circular standard increased gradually by 12%, on a bubble that lasted three hours, and the final value was still less than correct.

Willers* developed a graphical trial and error method for solving (2).

There is given below an account of an arithmetical trial and error method, developed by Thom+ for solving air flow problems, which was applied to a great variety of cases and found very convenient; for example, the Ψ values were found on an I section in 3 hours. This method has the advantage that it can be used to solve both (1) and (2).

2. Method of solution.

2.1. Description.- The boundaries are drawn to a suitable scale on squared paper, so that estimated Ψ values may be written at the corners of the squares. The process of estimating is given in the separate sections (3.1, 4.1, 5.1). For finding the value of Ψ at the centres of the squares, the following formula may be developed by Taylor's Theorem:-

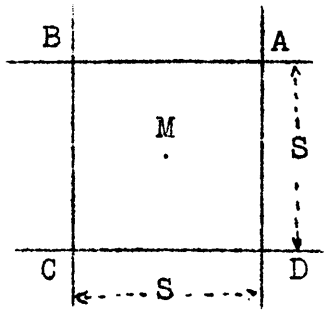

$$\Psi_M = \frac{1}{4}(\Psi_A+\Psi_B+\Psi_C+\Psi_D) - \frac{1}{8}S^2.\nabla^2\Psi - \frac{1}{384}S^4(\nabla^4\Psi + 4\frac{\partial^4\Psi}{\partial x^2.\partial y^2}) \quad \ldots\ldots\ldots (3).$$

Neglecting/

---

* Willers, Zeit. f. Math. u. Phys., Bd.55, 1907.

\+ Thom. Aero. Res. Comm., R.& M.1194.

T.3003
STRUT 9
FIG. 2.

TORSION OF 16"X6" B.S.1

Neglecting the terms with 4th order and higher derivatives and substituting for $\nabla^2\Psi$ from (1) or (2), the centre values are found throughout the section. Next, the same formula is applied to the centre values to find again the corner values, which are on the average a better approximation (2.2) than the original; so the process is repeated until the values cease changing, being now correct to the approximation of (3).

The method is illustrated in Fig. 2, which gives the solution for a 16 × 6" I section, while the typical convergence of the estimated Ψ values is shown at (a). Full numbers need not be used for every application of (3), but merely the differences, as shown at (a), thus lessening the work. Calculations with the full numbers are most suitably performed with a comptometer, which lessens the fatigue and chance of error. The last entered numbers at the foot of each column are obtained by a method given in (2.3) to shorten the process.

Two points may be noticed here. Firstly, the size of the square must be such that the neglected terms in (3) are really negligible. This is easily tested at any part of the section, when the values are settled, by enlarging that part, using smaller squares and finding if the values alter. Experience soon shows what smallness is needed, and this depends on the degree of accuracy required; for instance the results for the I section,

Fig. 2/

Fig. 2, with the size of the square shown, are less than 1% in error. Further, the parts which generally require testing are round portions of the boundaries which change direction quickly, such as internal corners. Thus the shaft with keyway (3.2) required two enlargements at the internal corner of the keyway to obtain the stresses accurately in this region.

Secondly, where a boundary does not pass through the corner of a square, the adjacent Ψ value must be found by interpolation; for 1% accuracy this may be done graphically but greater accuracy requires numerical interpolation, a short formula being developed for each point of the form

$$\Psi = a\Psi_1 + b\Psi_2$$

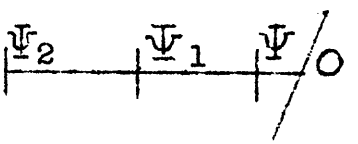

2.2. Convergence.- Let the size of the square be such that neglected terms in (3) do not affect the last significant figure. Let ε denote the error in Ψ; the estimated values are then $\Psi + \varepsilon$. In an ordinary round, finding the centre values from

$$\Psi_M + \varepsilon_M = \frac{1}{4}\sum\Psi + \frac{1}{4}\sum\varepsilon - \frac{1}{8}s^2.\nabla^2\Psi \quad \text{... from (3)}$$

since $$\Psi_M = \frac{1}{4}\sum\Psi \qquad - \frac{1}{8}s^2.\nabla^2\Psi$$

we have $$\varepsilon_M = \frac{1}{4}\sum\varepsilon \qquad \text{.....(4)}$$

where $\sum$ denotes the sum of the corner values.

Fig. 3a/

Fig. 3a shows the variation of Ψ and ε along a y = constant line and it is assumed for convenience of representation that Ψ does not vary with y. Fig. 3b, which gives ε alone, shows that the employment of (4) tends to smooth out abrupt changes in ε and to decrease it gradually. This point is also illustrated by finding a relation between ε and δ, where δ is the difference obtained in the estimated Ψ value by applying (3) twice, first for the centre value and again for the change in the corner value (a double round). If ε is the error at a corner, by writing its value at the surrounding corners in terms of its first and second derivatives and applying a double round, Fig. 4, the difference would be found in the form

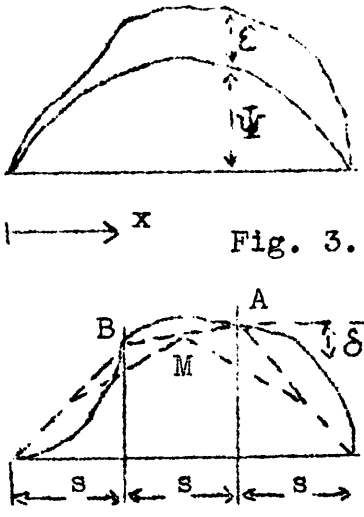

Fig. 3.

$$\delta = \frac{1}{4} s^2 . \nabla^2 \varepsilon \quad \ldots\ldots (5)$$

Fig. 4/

$$\delta = \tfrac{1}{4}\, S^2\, \nabla^2 \epsilon$$

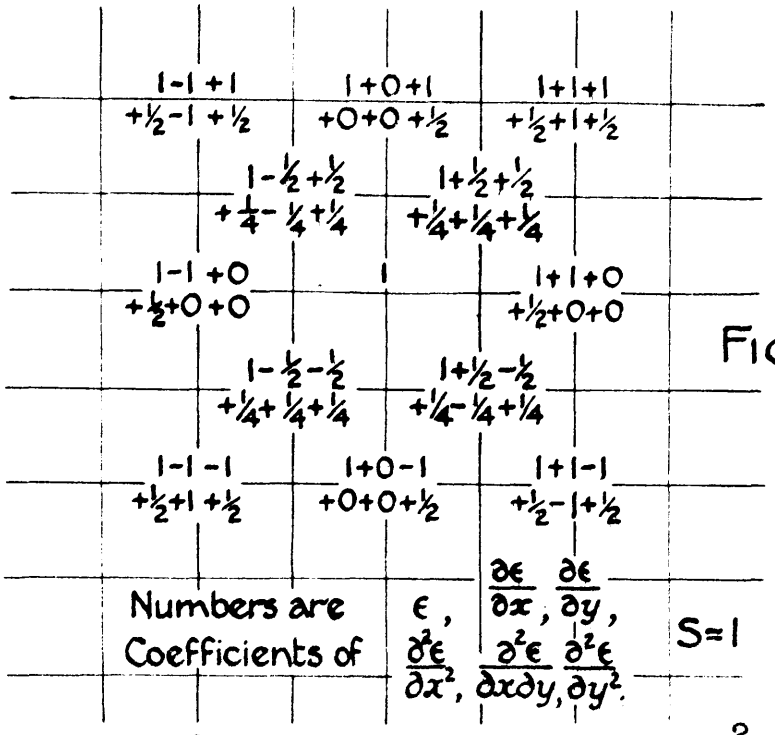

FIG. 4.

Thus when the $\mathcal{E}$-surface is concave up, $\nabla^2 \mathcal{E}$ and δ are +ve, that is, hollows fill up and also peaks flatten. This formula shows that the first tendency is to smooth out abrupt changes in $\mathcal{E}$, for in these regions $\nabla^2 \mathcal{E}$ has a high value, and the second tendency is to diminish $\mathcal{E}$ gradually over the section.

Further, the convergence is well tested by the variaty of cases tried, even the sharp internal corner of a hollow square, at which the stress is infinite, did not interfere with a definite solution.

2.3 Shortening the Process.- If an approximate average value of the ratio $\mathcal{E}/\delta$ could be estimated for a section, the slow creep of Ψ towards its correct value could be quickened since $\mathcal{E}$ is the required difference.

Consider/

Consider a rectangular portion of the section including $2m \times 2n$ squares of side s; assume that Ψ is known on the sides so that $\mathcal{E}$ there is 0. Let $\mathcal{E}$ take the simple form

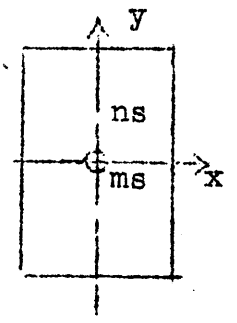

$$\mathcal{E} = \mathcal{E}_o \left(1 - \frac{x^2}{m^2 s^2}\right)\left(1 - \frac{y^2}{n^2 s^2}\right)$$

where $\mathcal{E}_o$ is the value of $\mathcal{E}$ at 0. From (5),

$$\delta = \frac{1}{4} s^2 . \nabla^2 \mathcal{E} = -\frac{1}{2} \mathcal{E}_o \left(\frac{1}{m^2} + \frac{1}{n^2} - \frac{x^2 + y^2}{m^2 n^2 s^2}\right)$$

$$\therefore \frac{\mathcal{E}_o}{\delta} = -\frac{2}{\frac{1}{m^2} + \frac{1}{n^2}} \quad \text{at } 0.$$

Owing to irregular variations in $\mathcal{E}$, δ is greater and $\mathcal{E}_o/\delta$ is less than the values given by this expression. It is found that using

$$\frac{\mathcal{E}}{\delta} = -\frac{1.5}{\frac{1}{m^2} + \frac{1}{n^2}} \quad \ldots\ldots\ldots (6)$$

all over the section gives good results in practice. The best procedure is to take two double rounds, applying (6) to the differences of the second.

In/

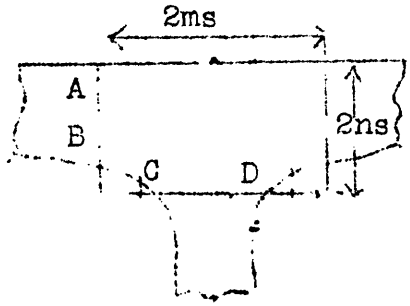

In actual cases which are not rectangular, equivalent values of m and n are used; for example in an I section the equivalent rectangle is as shown, the error being assumed zero at AB and CD, since Ψ may be fairly accurately estimated there by the formula for long thin sections (3.1).

Example. 16 × 6" I, Fig. 2; m = 3, n = 2.5, $\varepsilon/\delta = -6$ The centre point in (a), $\Psi + \varepsilon_1 = 19$, 1st double round $\delta_1 = 0.2$, 2nd, $\delta_2 = 0.4$, therefore 2nd approx. $\Psi + \varepsilon_2 = 19 + 0.6 + 6 \times 0.4 = 22$, (correctly 23.1).

The formula (6) is very useful and makes this method, otherwise laborious for this type of work, practicable.

3. Solid Sections.

3.1. Application of the above method.- In the case of prisms with solid sections, the first point to consider is the estimation of the maximum Ψ values, for once these are found intermediate values may be guessed by drawing smooth curves. On a long rectangle, except at the ends, we may assume $\partial\Psi/\partial y = 0$ so that (1) becomes

$$\frac{\partial^2\Psi}{\partial x^2} = -2$$

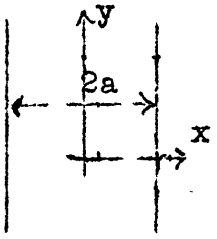

Integrating $\Psi = a^2 - x^2$

and $\Psi_{max.} = a^2$ where $x = 0$.

This/

This holds for any parallel sided part, such as the web of an I section and also for a gradually tapering part like the flange.

The maximum Ψ value on a circle of radius a, is found by transforming (1) to polar coordinates giving

$$\frac{\partial^2\Psi}{\partial r^2} + \frac{1}{r} \cdot \frac{\partial\Psi}{\partial r} + \frac{1}{r^2} \cdot \frac{\partial^2\Psi}{\partial\theta^2} + 2 = 0$$

Here $\frac{\partial\Psi}{\partial\theta} = 0$ so that $\frac{\partial}{\partial r}\left(r \cdot \frac{\partial\Psi}{\partial r}\right) + 2r = 0$

$$\therefore \quad \Psi = \frac{1}{2}a^2 - \frac{1}{2}r^2 \quad \text{and} \quad \Psi_{max.} = \frac{1}{2}a^2$$

For I or L sections the formula

$$\Psi_{max.} = \frac{1}{2}a^2 + 0.27\,(b_1^2 + b_2^2 + b_3^2 + \ldots)$$

may be used,

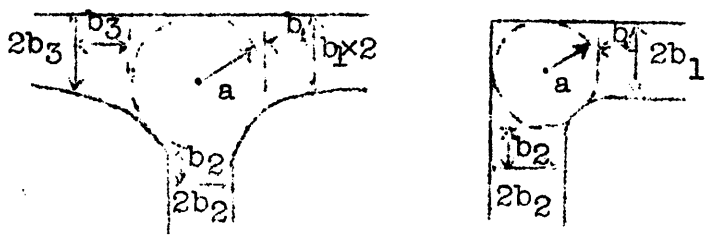

The torsional properties of a prism are expressed by torque $T = N\tau \cdot C$, stress $q = N\tau \cdot R$ where C

is/

is a quantity of the fourth, and R, the stress factor, of the first degree in the linear dimensions of the cross section. The relation between T and q is

$T = q \cdot \frac{C}{R}$. Now $C = 2\int\int \Psi . dx . dy$, which is easily evaluated since Ψ is known throughout the section.

To find the stresses at any point on the section involves finding

$$R = \sqrt{\left(\frac{\partial \Psi}{\partial x}\right)^2 + \left(\frac{\partial \Psi}{\partial y}\right)^2}$$

This is done most easily and accurately by difference formulae. The value of $\partial \Psi / \partial x$ at the corner of a square is given by

$$S \cdot \frac{\partial \Psi}{\partial x} = \Delta\Psi - \frac{1}{2}\Delta^2\Psi + \frac{1}{3}\Delta^3\Psi - \frac{1}{4}\Delta^4\Psi \ldots.$$

or more generally, for a point B on the boundary not at the corner of a square

$$S \cdot \frac{\partial \Psi}{\partial x} = \Delta\Psi - \frac{2x+1}{2}\Delta^2\Psi + \frac{3x^2 + 6x + z}{6}\Delta^3\Psi$$

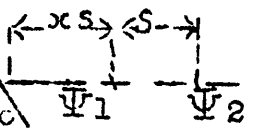

where $\Delta\Psi$, $\Delta^2\Psi$ are the first, second ------ differences of a table of values, whose leading term is Ψ_1, second , Ψ_2, etc.

A/

A check may be applied to solutions for the solid sections obtained by noticing that the distortion φ, of the material parallel to the axis must be single valued.* Hence round any closed curve in the section

$$\int \frac{\partial \varphi}{\partial s} \cdot ds = 0$$

and also

$$\int \frac{\partial \psi}{\partial n} \cdot ds = 0$$

where ψ is the function conjugate to φ and n is the normal to the curve. Again $\Psi = \psi - 1/2(x^2 + y^2)$

$$\therefore \int \frac{\partial \Psi}{\partial n} \cdot ds = \int \frac{\partial \psi}{\partial n} \cdot ds - \int r \cdot \frac{\partial r}{\partial n} \cdot ds$$

$$= 0 - \int r.\cos(\theta,s) \cdot ds$$

$$= -\int r^2 \cdot d\theta = -2A \quad \ldots (7)$$

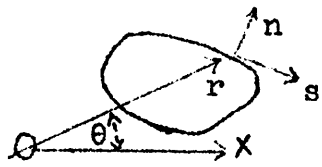

where A is the area enclosed by the curve. Taking the boundary as the curve, $\partial \Psi / \partial n = R$, the stress factor, and the relation (7) expresses the fact that the area under the stress factor curve, plotted on the boundary, equals twice the area of the section. This check has been applied to most of the solutions,

3.2 Results.- The torsional properties of several British Standard structural sections were solved

and/

---

* Taylor and Griffith, Aero. Res. Comm., R.& M.392.

and the results checked by direct test, as shown in Table I. There is also given the properties as obtained by three approximate formulae, one developed by the author (C_1), one due to Griffith,* and the third to Weber.×

Table I.

Values of C and $R_{max.}$, shown $\begin{cases} C \\ R_{max.} \end{cases}$

Section	Analysis	Direct Test	Approximate Formulae		
			C_1	Griffith C_2	Weber C_3
B.S.16 × 6"I	2.28 1.16		2.29	1.18	
B.S.5 × 4½"I	0.574 0.84		0.572	0.683 0.87	0.496
5 × 4½"I		0.390	0.386	0.457 0.77	0.342
B.S.6 × 3"I			0.167	0.197 0.63	0.143
6 × 3"I		0.153	0.150	0.180 0.62	0.128
B.S.4 × 3"I			0.135	0.166 0.61	0.113
4 × 3"I		0.111	0.112	0.132 0.57	0.098
B.S.6 × 3"[			0.163	0.179 0.56	0.143
6 × 3"[		0.167	0.164	0.56	0.147
B.S.12 × 4"[	0.905 0.84		0.914	1.010 0.82	0.823
B.S.2 × 2"L × 3"	0.0344 0.447		0.0346	0.0372 0.445	0.0317
2 × 2"L × 0.321"		0.0449	0.0454		0.0404

* Griffith, Aero. Res. Comm., R.& M.334.

× Weber, Z.V.d.I. Bd.66, 1922, pp.764-769 (abstract), also Mechanical Engineering, V.44, 1922 (abstract).

The sections for which a solution is obtained by analysis have dimensions given in the B.E.S.A. tables whereas the actual sections tested have dimensions somewhat different from these. Yet the approximate formula (C_1) supplies the link and shows that the test results are in agreement with the analytical solutions.

The valuo C_1 is obtained by dividing the section into rectangles and wedges, the basis for which is indicated in (3.1), where it is shown that parallel-sided and gradually tapering parts have the same Ψ values as when they are separated from the section. Now this holds throughout a section except at the junctions, and there special treatment is necessary. Weber, using this method of dividing into rectangles and wedges, obtained

an/

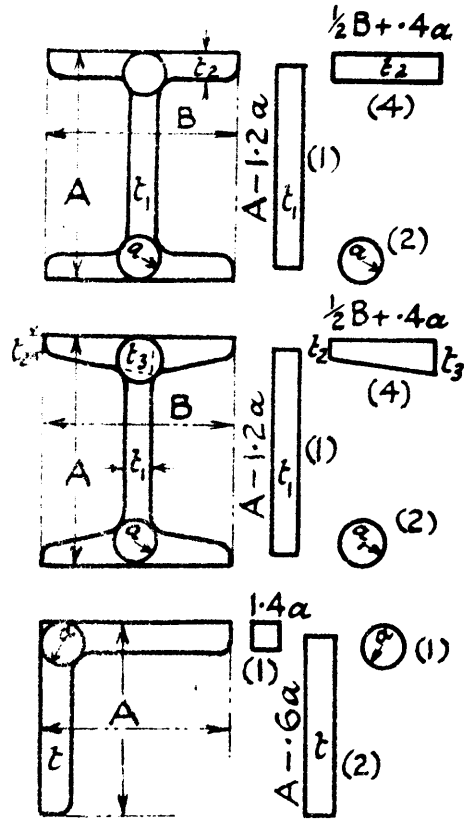

FIG. 10.

an expression for the junctions by approximate analysis which gives low results as shown (C_3).

To obtain C_1 - draw in the largest circle at a junction, radius a. Continue the boundaries of the parallel-sided or wedge portions to a distance 0.4a past the centre of the circle. Thon $C_1 = \sum C$ for the separate circles, rectangles and wedges. Thus for an I section with flanges of constant thickness, Fig. 10a, the separate parts are:-

2 circles radius a

1 rectangle, $(A - 1.2a) \times t_1$

4 rectangles, $(B/2 + 0.4a) \times t_2$

In using the above formula, the value of C for rectangles may be found from tables, or from

$$C = \frac{1}{3} bt^3 - 0.21\, t^4 \quad \text{correct to}$$

1/2% for $b/t > 2$, ... (8)

where b = breadth, t = thickness.

For a wedge, as in (3.1), since $\partial^2\Psi/\partial y^2 \doteq 0$ on strip $t \times dy$, $\Psi = (1/2\ t)^2 - x^2$, with the origin at the centre of thickness.

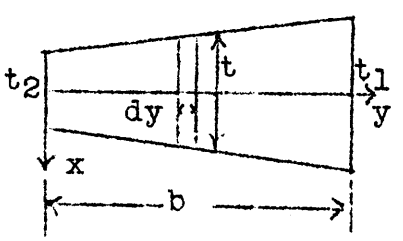

$$C = 2\int_0^b dy \cdot 2\int_0^{1/2t} \Psi \cdot dx = \int_0^b 1/3t^3 \cdot dy = \frac{b}{12} \cdot \frac{t_1^4 - t_2^4}{t_1 - t_2}$$

The correction for the ends is obtained from (8), and gives

C =/

$$C = \frac{b}{12} \cdot \frac{t_1^4 - t_2^4}{t_1 - t_2} - 0.1\,(t_1^4 + t_2^4)$$

For $R_{max.}$, Griffith's empirical formula gives good results for these sections.

The stress factor R is plotted round the boundaries of the B.S.5 × 4-1/2", I, and the B.S.2 × 2 × 0.3"L, Figs. 12, 13. As shown in (3.1) the area under these curves supplies a check to the solution. The stresses on the flange face and the web of the 5 × 4-1/2", I and the 6 × 3" [, were found by means of tensometers, (see 3.3) the results agreeing well with analysis (within 5%). Fig. 14 illustrates the experimental and analytical stresses for the flange face of the I section.

A shaft with keyway has also been solved by analysis. The dimensions are those of standard practice and the radius at the internal corner of the keyway is taken equal to that on a shaft tested by Gough,* so that the results of analysis could be compared with the test results. Two enlargements were required at the internal corner and Fig.15 gives the complete solution as illustrating the method. Also the curve of stress factor round the boundary is given in Fig.16.

Results/

---

* Gough, Aero. Res. Committee, R.& M.864.

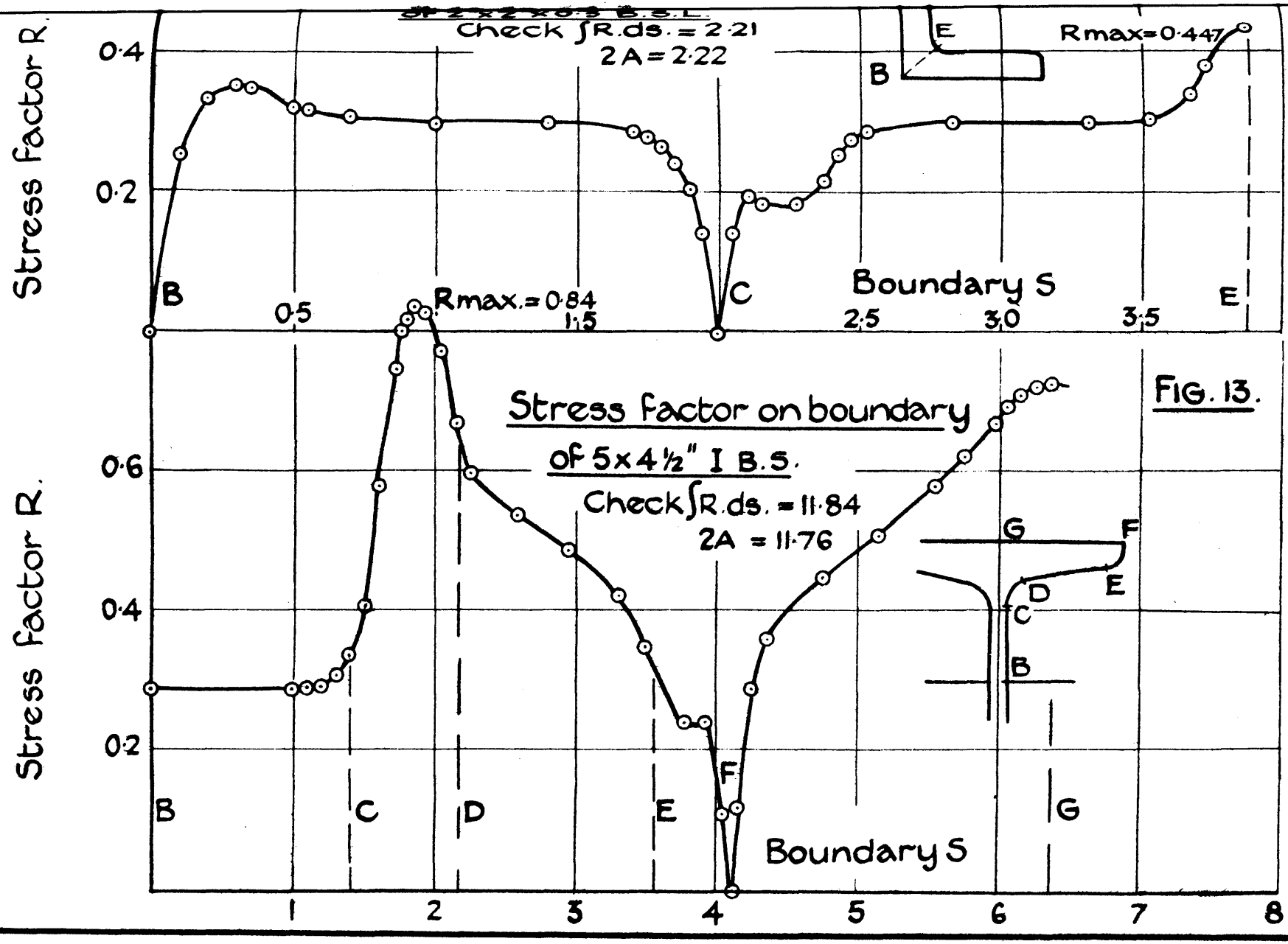

FIG. 13.

T.3003.
STRUT 9.
FIGS. 12, 13.

T. 3003.
Strut 9.
Fig. 14.

STRESSES ON FLANGE FACE OF 4½" I SECTION, WHEN TORQUE = S TONS-INS.

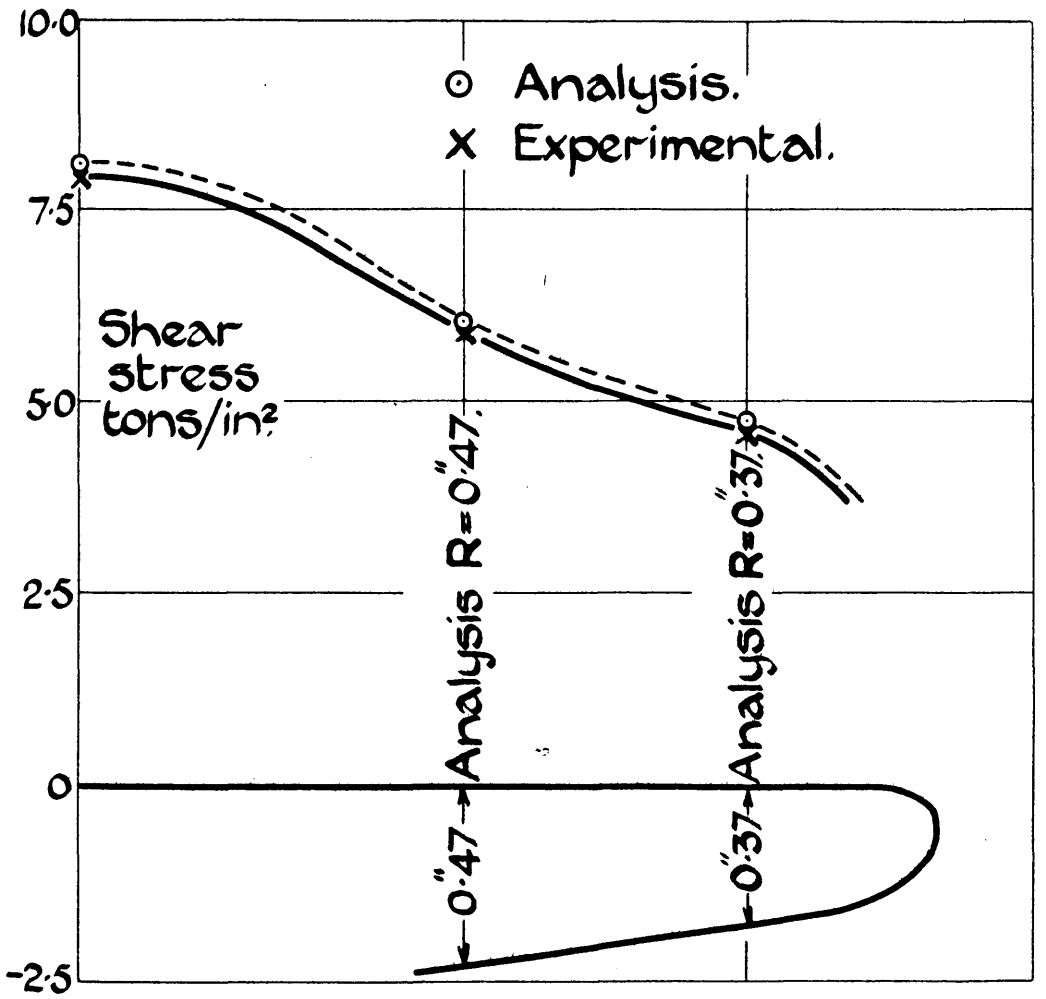

Results. Rad. = 10.
Analysis C = 14,300; $R_{max.}$ = 17.8; R_1 = 12.4

Gough's tests C = 14,300 and 13,900

Griffith's formula C = 14,600; R_1 = 11.7
where R_1 is the stress at the centre of keyway.

3.3 Tests.- Torsion tests on the structural sections were carried out using a 100 T capacity Buckton testing machine. Twist was measured by two mirrors, whose frames were pinned at the centre of the flange faces, and two telescopes, sighting on scales reflected in the mirrors. The distance between specimen and scale was 274", and the scales could be read to 1/50", allowing a high degree of accuracy. Fig. 17 shows the grips for the I and [sections. At first the key pieces were fastened to the flanges by three pins, but the torque-twist curves produced had large loops, due to the end constraining actions preventing the centre lines of the flanges from taking up their positions on a helix, and thereby applying a transverse bending moment. This trouble was completely surmounted by having only one pin, connecting grip to flange, and free to turn in the grip, and by having the surfaces well greased to eliminate friction.

Typical torque-twist curves are shown in Fig.18

In order to measure the stresses on the specimens Huggenberger Tensometers of gauge length 1" and (1/2") were used. Since the scale can be read to 0.02" and the magnification is 1200, the stresses are measured to 0.2 tons per in.^{2}. To determine the shear stress at any point, strain

readings/

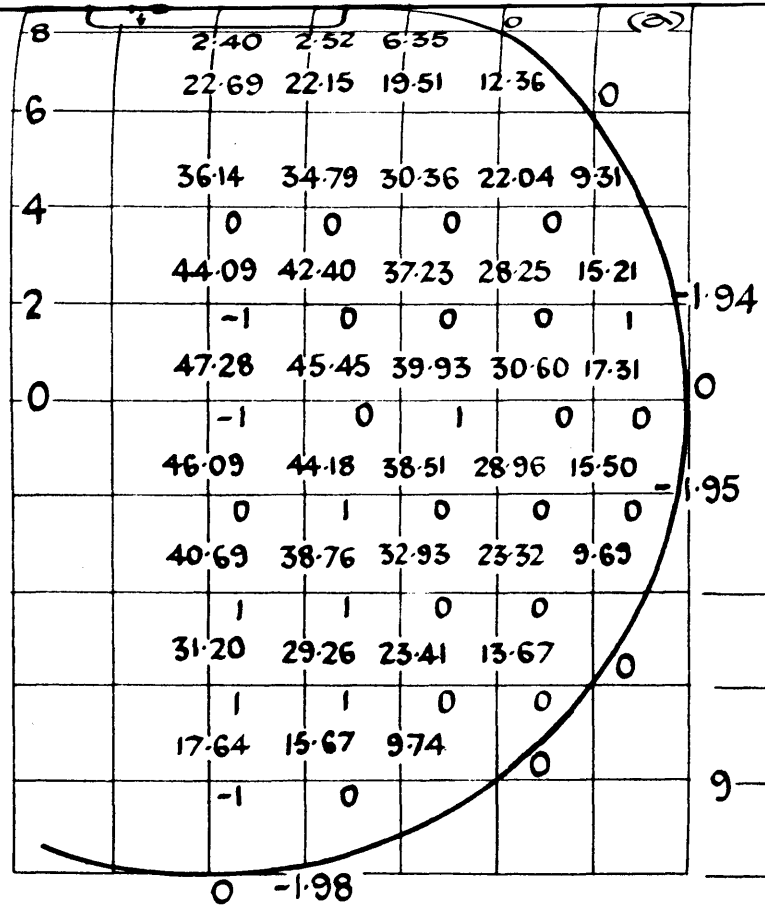

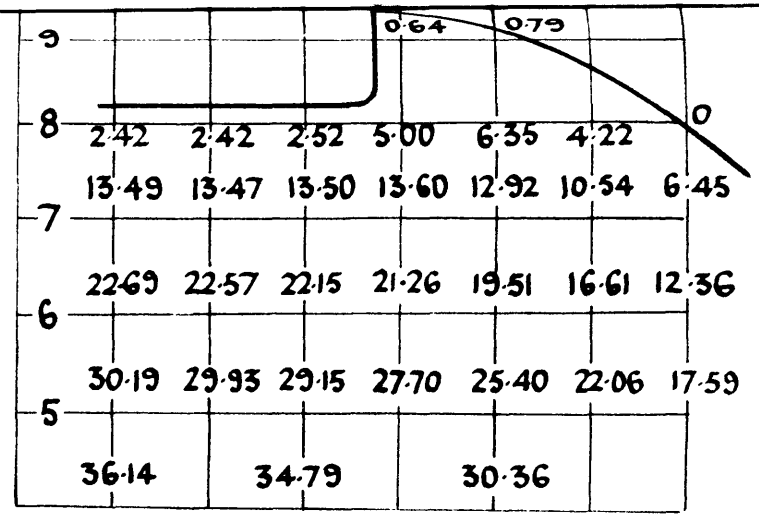

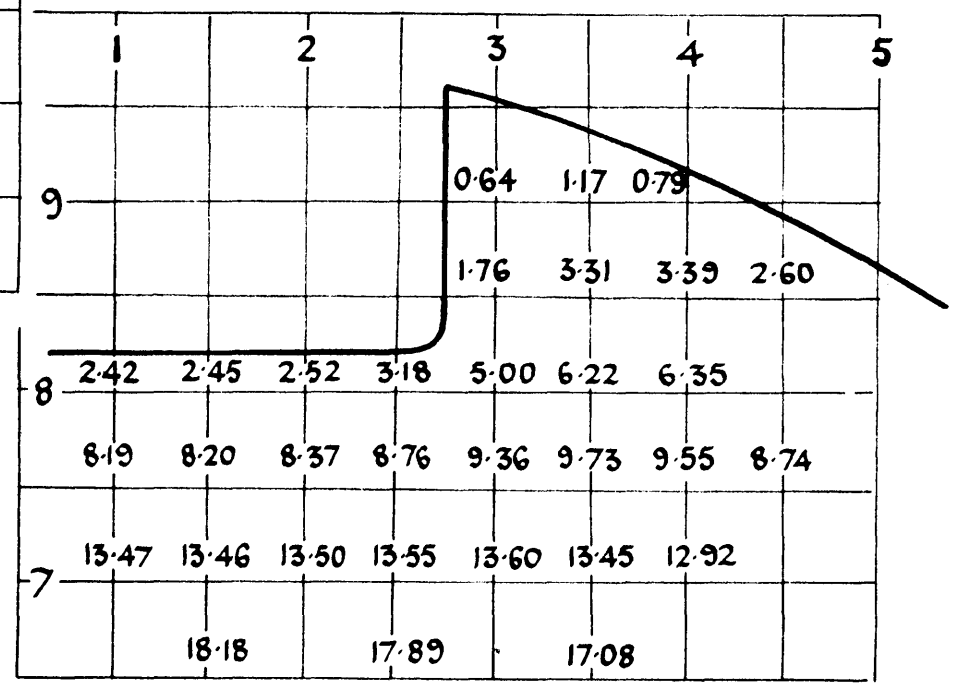

Keyway ed Shaft, Rad. = 10

Solution of $\nabla^2\Psi + 2 = 0$

Formula $\Psi_M = \frac{1}{4}(\Psi_A + \Psi_B + \Psi_C + \Psi_D)$

+ 1 --- for (a)

+0·25 -- for (b)

+0·06 -- for (c)

T.3003.
STRUT 9.
FIG. 15.

T. 3003.
Strut 9.
Fig. 16.

KEYWAYED SHAFT, RAD. = 10
STRESS FACTOR ON BOUNDARY.

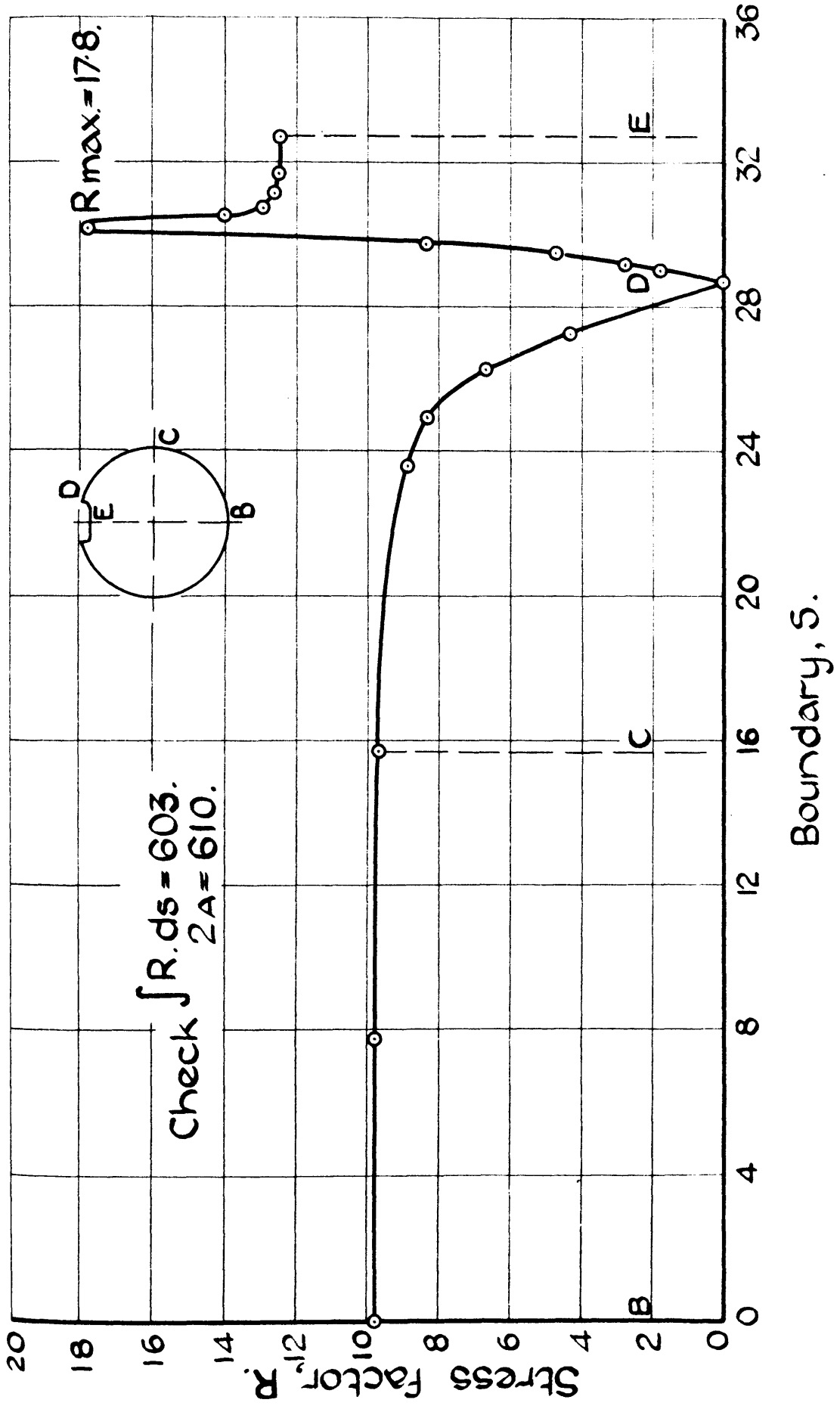

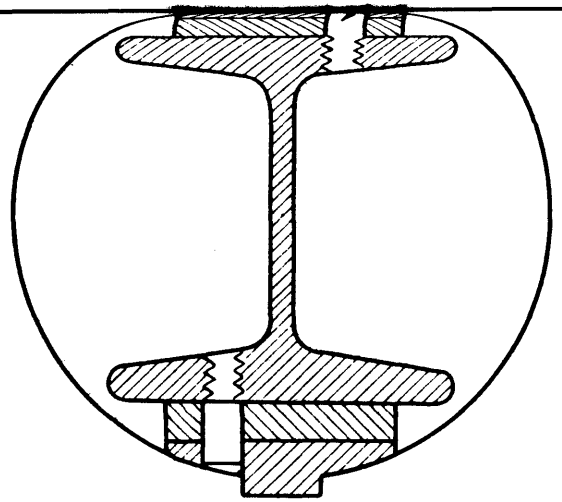

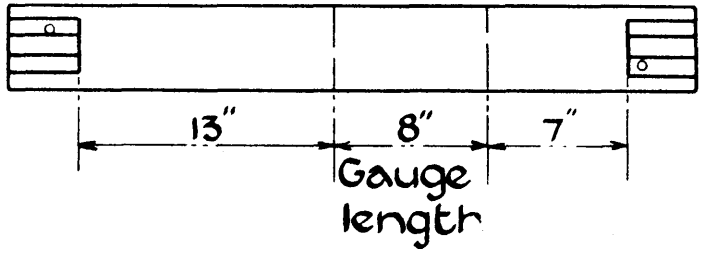

GRIPS FOR STRUCTURAL SECTIONS.

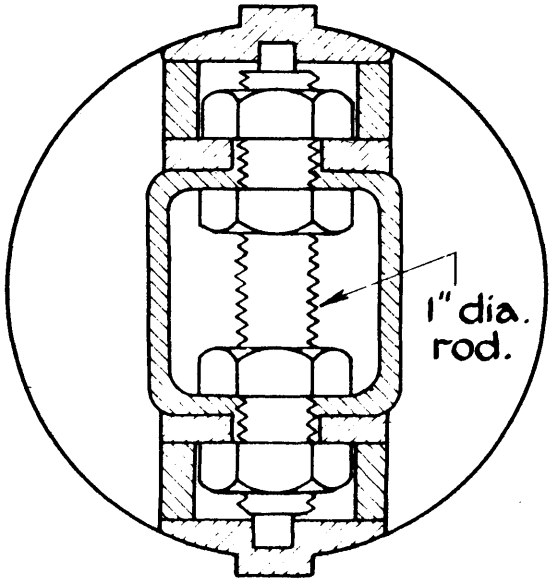

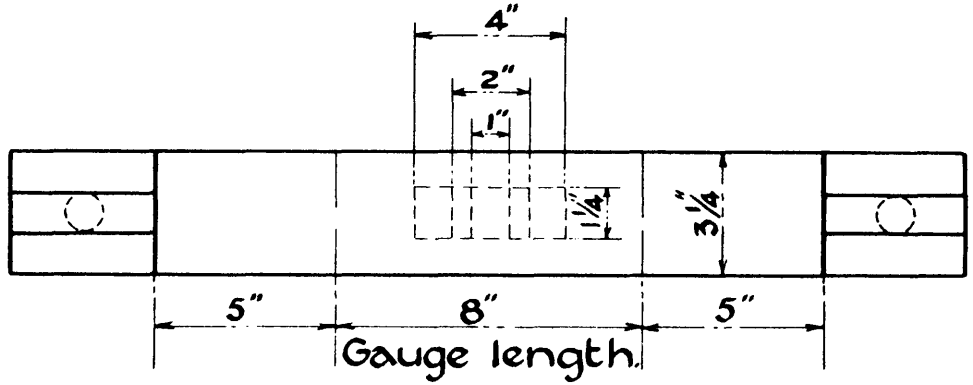

GRIPS FOR 3¼" SQUARE TUBES.

T.3003.
Strut 9.
Fig. 17.

readings are taken on two directions at 45° to this stress, AB and CD in Fig.19. If e is the strain,

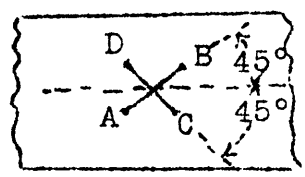

Fig. 19.

shear stress $q = \frac{Ee}{1 + \sigma}$, where σ = Poisson's ratio.

A second use found for the instruments was the study of end effects, the stresses being found close to the grips. There was no appreciable difference at a distance of half the flange breadth from the edge of the grip and this was checked by moving one mirror to this position, and finding the twist on the new gauge length.

At an internal sharp corner the stress by calculation becomes infinite. Actually, as is well known, local yielding relieves this high stress. Yet it was thought worth while removing the fillet at the junction of flange and web in the case of two I sections and testing this altered section. The result was that no difference could be detected in the torque causing failure, as shown in table 2.

There were three test specimens for the same size of section, one being used for the test to failure, the second for the test with the fillet removed, and the third cut up into specimens. These specimens were circular and rectangular and were taken from the positions shown in Fig.20. Using a single lever torsion testing machine, and telescope and mirror apparatus, the rigidity modulus N, and the torque at failure were found for the specimens.

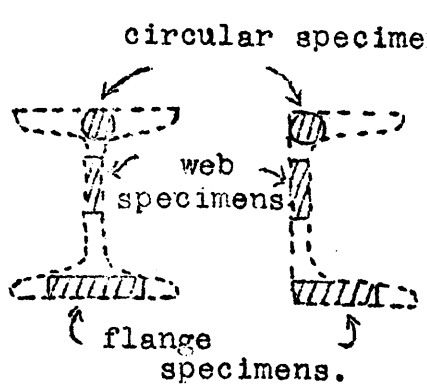

Fig. 20.

The/

The value of N varied from 11.62 - 11.79 × 10^6 lb./in^2 so the average value N = 11.7 × 10^6 was used.

In calculating the stresses from the tensometer tests it is necessary to know Young's modulus, E, and Poisson's ratio, σ; these were found by subjecting the rectangular specimens to tension in order to measure the longitudinal and transverse strains. The results are

$$E = 30.5\ 10 \text{ lb./in.}^2 \qquad \sigma = 0.30$$

Again, calculating σ from $E = 2N(1 + \sigma)$, gives $\sigma = 0.30$

3.4 Failure.- Most parts of construction, subjected to torsion are considered to have failed when they take a considerable permanent set. For ductile materials like mild steel this is the criterion in the case of steady stresses. Fig.21 shows a typical torque-twist curve for a circular specimen of mild steel. After the elastic limit is passed the curve varies for different specimens, sometimes showing a definite yield, as at (a), or no definite yield, as at (b). This depends on the rate and manner of loading, and on the heat and mechanical treatment the material has received. Because of this indefiniteness, it would seem better to use a limit of proportionality or a torque giving a definite permanent twist, as the basis of failure, in preference to a yield point. Now the limit of proportionality is too severe a basis and very indefinite, since with accurate twist measuring arrangements it can be taken at

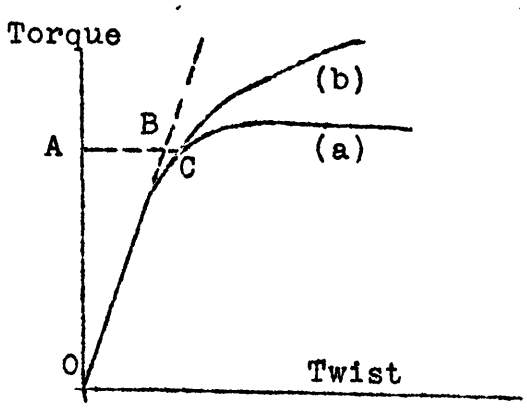

Fig. 21.

nearly/

nearly zero torque.* On these considerations it was decided to use a proof torque as the basis of failure, defining it as the torque producing a deviation from the elastic line of 10% of the elastic twist at that torque. In Fig.21 the proof torque is OA, producing BC = $\frac{1}{10}$ AB. This basis was considered as also suitable for complicated sections as the curves are of the same form, Fig.18.

In the tests on the structural sections, it was found that the calculated maximum stresses at proof torque, were considerably higher than the corresponding maximum stresses of the specimens, the calculations assuming perfect elasticity. This is shown in column 6 of table 2. Thus local high stresses do not have as much effect as would be anticipated from analysis. So the effective maximum stress is less than the calculated, and a formula consistent with the results of these tests is

$$R_{eff.} = R_{mean} + \frac{1}{6} (R_{max.} - R_{mean}) \quad \ldots\ldots\ldots (9)$$

where R_{mean} is the mean stress factor on the boundary and equals $R_{mean} = \frac{2A}{P}$, A = area of section, P = length of boundary. Column 7, table 2 gives the results of this formula.

Table 2./

---

*Guest and Lea, P.R.S. 93, 1916-17.

Table 2.

Specimen	C	Stress factor		Proof Torque T	Stress	
		$R_{max.}$	$R_{eff.}$		$q_{max.}$	$q_{eff.} = T/C \cdot R_{eff.}$
	in.^{4}	in.	in.	tons/in	tons/in^2	tons/in^2
6 x 3 I	0.155	0.60	0.37	5.2	20.1	12.4
6 x 3 I, fillets removed	0.147	high		5.1		
Circle 0.500" diameter.	0.00616	0.25	0.25	0.283	11.5	11.5
Flange rect. 2.01 x 0.288	0.0146	0.29	0.26	0.70	13.9	12.5
Web rect. 2.02 x 0.276	0.0129	0.28	0.25	0.70	15.2	13.6
6 x 4-1/2 I	0.390	0.74	0.46	8.4	15.9	9.9
6 x 4-1/2 I fillets removed	0.376	high		8.7		
Circle 0.643" diameter	0.0168	0.32	0.32	0.52	9.9	9.9
Flange rect. 2.02 x 0.475	0.0620	0.475	0.40	1.46	11.2	9.4
Web rect. 2.01 x 0.282	0.0136	0.28	0.26	0.70	14.4	13.4
6 x 3 [	0.167	0.56	0.36	4.8	16.1	10.4
Flange rect.	0.0400	0.425	0.35	1.16	12.3	10.2
Web rect.	0.0104	0.26	0.24	0.58	14.5	13.4
6 x 3 I	0.111	0.57	0.35	3.6	18.5	11.0
6 x 2 x 0.32 L	0.0449	0.50	0.33	1.5	16.7	11.0

It will be noticed that the web specimens show higher stresses than the others, but this does not interfere with the consistency of the results since, as is shown in Fig. 13, the material which fails in a structural section is the flange at the junction of the web, the region from which the circular and flange rectangular specimens are taken.

4./

4. Hollow Sections.

4.1. Application of the Analytical Method.- We cannot proceed directly with the solution since there are two boundaries and the constant for one of them is unknown. If its value is estimated, and a solution obtained, equation (7) should be satisfied, on both boundaries. The amount and sign of the error in (7) gives approximately the necessary correction to the unknown constant. So the procedure is to solve (1) with one boundary constant estimated, next to correct the constant from the solution, and then to solve (1) again with the new value. Usually two solutions are sufficient and it should be noticed that the second is quite short since the Ψ values by a regular alteration of those of the first solution, are nearly correct.

Thus for the hollow square, 30 × 30" outside, and 3" thick (see 4.2), taking the outer boundary constant $B_2 = 0$, the inner by estimation $B_1 = 48$, the solution gives

$$\int R_2 \, .ds = 2040 \qquad 2A_2 = 1800$$

Length of outer boundary = 120, so R should be diminished on the average by 2. Now, since R is the slope of Ψ and the thickness is 3, the corrected value of B is 48-2 × 3 = 42. Similarly from the second solution a third approximation to B_1 is 42.4, and hence it is not necessary to proceed with the third solution for accuracy within 1%.

The/

The formula for C is

$$C = \iint \left\{ \left(\frac{\partial \Psi}{\partial x} \right)^2 + \left(\frac{\partial \Psi}{\partial y} \right)^2 \right\} . \, dxdy = \int \Psi . \frac{\partial \Psi}{\partial n} . \, ds - \iint \Psi . \nabla^2 \Psi . dx . dy$$

where the single integral is taken round the boundaries, and the double integral over the section.

$$\therefore \quad C = 2A_1B_1 - 2A_2B_2 + 2 \iint \Psi . dx . dy$$

where A_1, A_2 are areas enclosed by inner and outer boundaries and B_1, B_2 are the inner and outer boundary constants.

4.2 Thin Tubes.- An approximate solution is easily obtained*, giving

$$T = 2Aqt = \frac{4A^2t}{l} . N\tau . \quad \ldots\ldots (10).$$

where A is the area, and l the length of the mean line midway between the boundaries, and t is the thickness.

The only experimental work done on tubes, other than circular, that could be traced, was by Vedeler× and the results he obtained showed that the angle of twist up to twice that given by (10). He explained this by the

discontinuity/

---

* Case, Strength of Materials.

× Vedeler, Trans. Inst. Nav. Arch., 1924.

discontinuity at the corners. So it was decided to find the properties of a hollow square both by analysis and by test.

The analysis was taken on a hollow square, 30 × 30 outside, 3 thick. When the outer boundary constant $B_2 = 0$, the inner $B_1 = 42.4$. The stresses on the boundaries are given in Fig. 22.

The checks $\int R_2 \cdot ds = 1801$, $\int R_1 . ds = 1151$

$2A_2 = 1800$, $2A_1 = 1152$

By analysis $C = 63,000$

By the approx. formula, $C = 59,000$

Thus even for this moderately thick tube the error in the approximate theory is small.

In the tests it was thought well to avoid riveted or welded joints, and therefore solid drawn circular tubes, hammered to square form were used. The dimensions were 3-1/4 × 3-1/4" outside and two thicknesses 0.172" and 0.233". They were annealed to remove initial stress as far as possible. The tests were taken in a similar manner to those on the structural sections, although a much more rigid type of grip was found necessary, as shown in Fig. 17. The twist was measured and the stresses checked by tensometers. There was fair agreement between these results and the approximate formula (10), 5% being the maximum difference in the twist and 10% in the stress.

Therefore/

T. 3003.
Strut 9.
FIG. 22.

STRESS FACTORS ON BOUNDARIES OF HOLLOW SQUARE. 30 x 30 x 3.

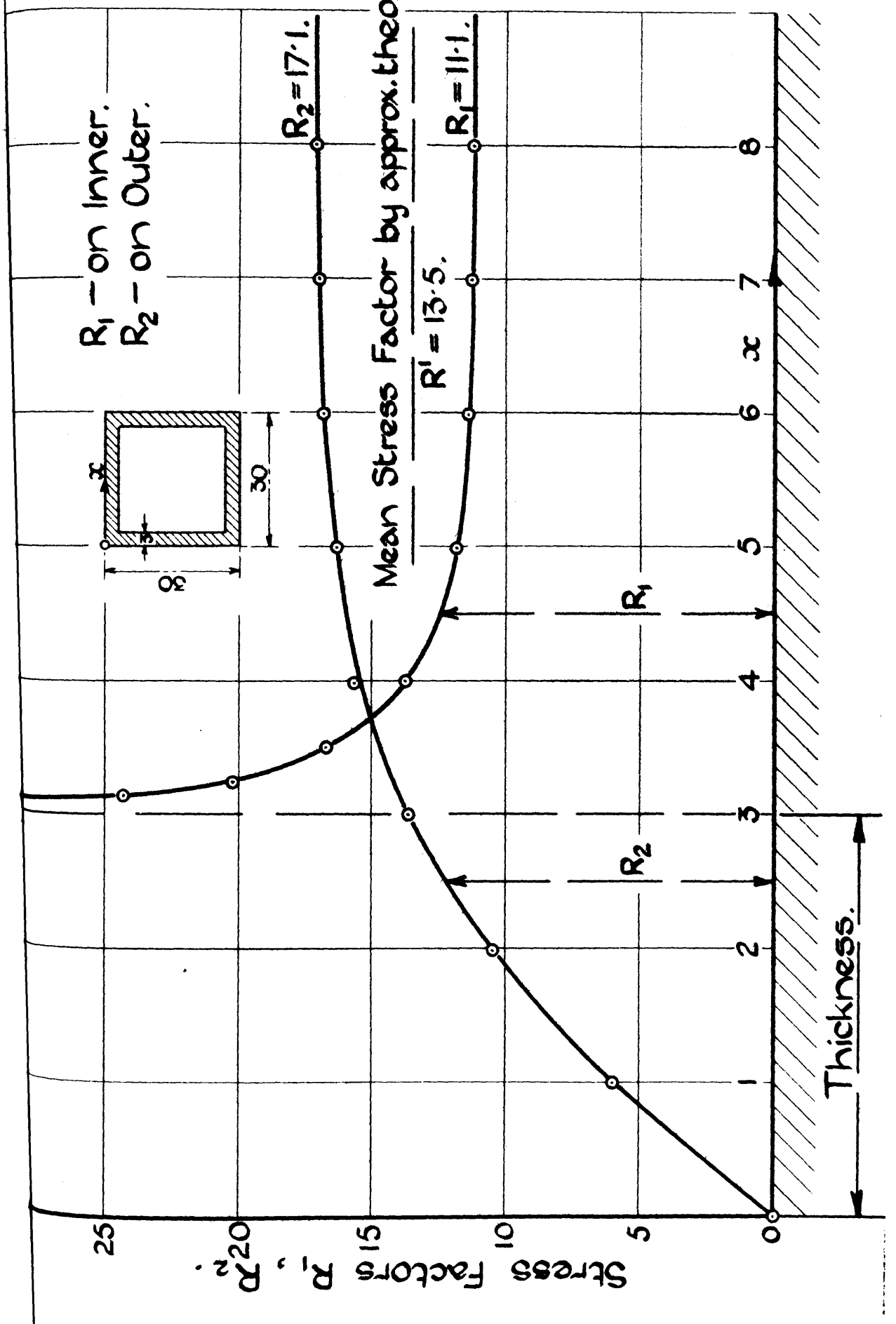

Therefore (10) gives sufficiently accurate results for tubes of the above order of thickness. Vedeler's high twist values could be explained by slipping at the riveted connection in his test specimen.

An interesting point investigated was the effect of a discontinuity in the form of a rectangular hole, cut in one side of the tube. Fig. 17 shows the position and size of the holes. The procedure was to take a test with the shortest length of hole, then to increase the length and re-test. This was done on tubes of two thicknesses and the results gave the percentage increase in twist as independent of the thickness. Also the increase in twist was proportional to the length of the hole, for lengths less than 3", and could be expressed in the form -- length l including the 1-1/4" hole of length l' ($l' < 3"$), has the same angle of twist per unit torque as length $(l + 0.7l')$ of the uncut tube.

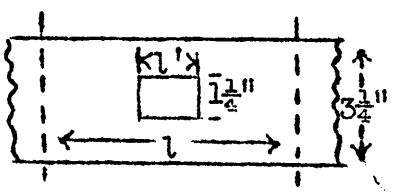

The stresses were measured at the corners of the holes with the tensometers using 1/2" gauge length. The maximum tensile stress lay between 3.5 and 4 times the tensile stress in the uncut tube and was also independent of the thickness. This agrees with the concentration factor for a circular hole in a flat plate subjected to shearing stresses.

4.3/

4.3 Hollow Serrated Shaft.- The evaluation of the torsional properties of the hollow serrated shaft, shown in Fig. 24, introduces a departure from the usual method. As there is symmetry it is only necessary to solve the part of the section of sector shape, including a half serration, ABCD. By conformal representation, this sector can be transformed into a rectangular shape as shown, A'B'C'D', Fig. 23, which is more suitable when applying the analytical method.

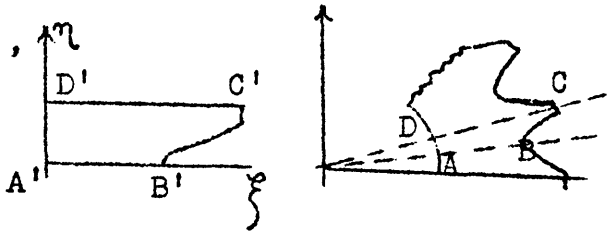

Fig. 23.

The formula of transformation is

$$\xi + i\eta = m \log (x + iy) = m \log r + mi\theta$$

$$\therefore \left.\begin{aligned} \xi &= m \log r \\ \eta &= m\theta \end{aligned}\right\} \quad \ldots\ldots\ldots\ldots\ldots\ldots (11)$$

where m has any convenient value and is chosen to make A'D' an exact number of units. The new boundary A'B'C'D' is found using (11), and noticing that at B' there is a circular arc of radius m log 4.49/4.39, for in this type of representation infinitesimal elements are similar.

It may be shown that

$$\frac{\partial^2 \psi}{\partial x^2} + \frac{\partial^2 \psi}{\partial y^2} = \frac{m^2}{r^2}\left(\frac{\partial^2 \psi}{\partial \xi^2} + \frac{\partial^2 \psi}{\partial \eta^2}\right)$$

Now the torsional properties are found by solving either

$\partial^2\Psi/$

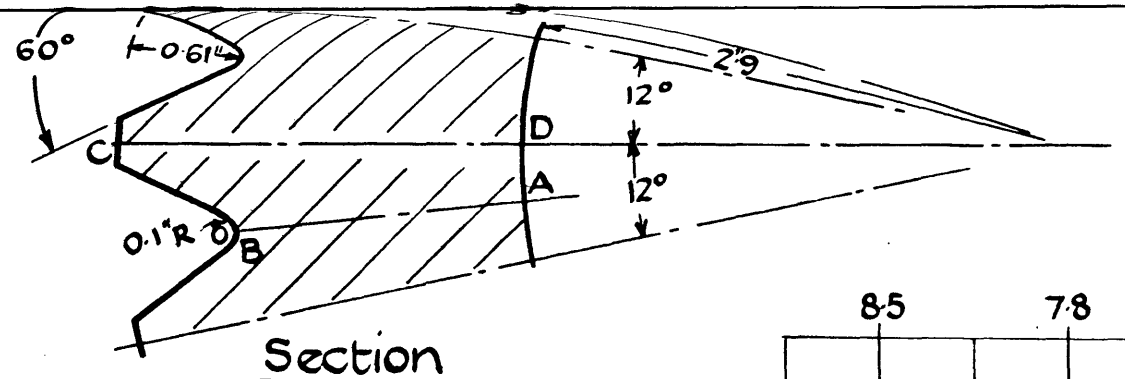

Section

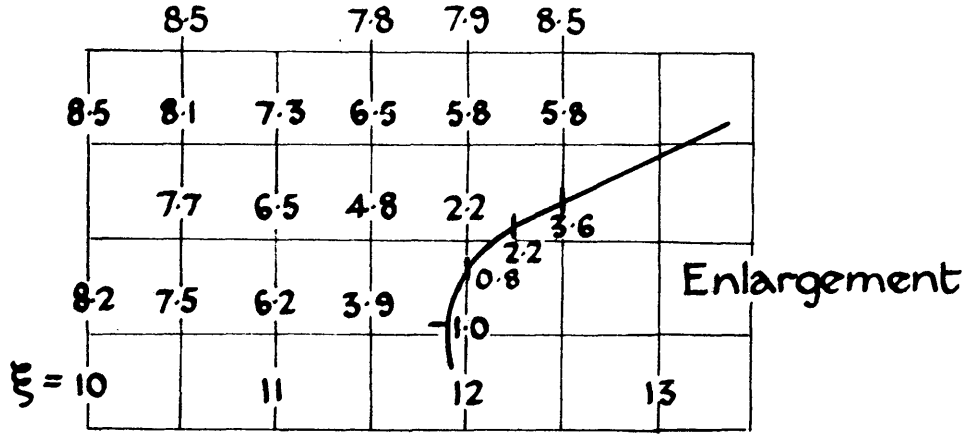

Enlargement

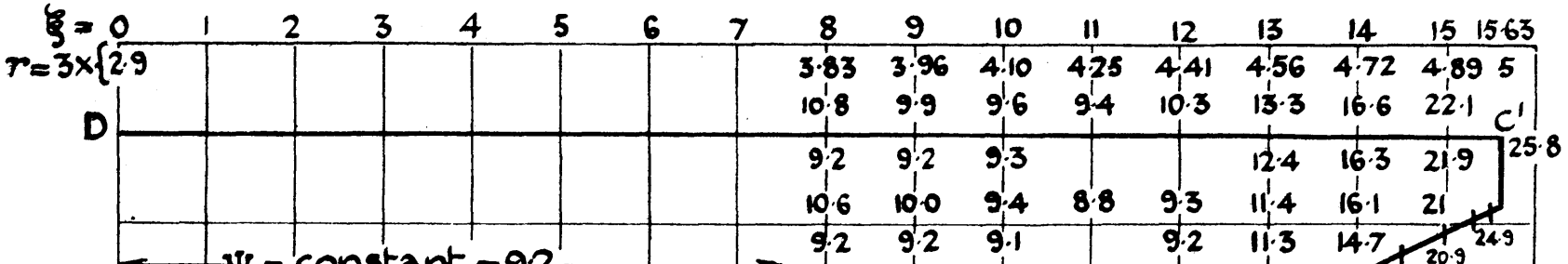

Transformed field.

T.3003.
STRUT.9.
FIG 24.

$$\frac{\partial^2 \Psi}{\partial x^2} + \frac{\partial^2 \Psi}{\partial y^2} + 2 = 0 \quad \text{or} \quad \frac{\partial^2 \psi}{\partial x^2} + \frac{\partial^2 \psi}{\partial y^2} = 0$$

where $$\Psi = \psi - \frac{1}{2}(x^2 + y^2)$$

Thus it is simpler to use ψ in this case since

$$\frac{\partial^2 \psi}{\partial \xi^2} + \frac{\partial^2 \psi}{\partial \eta^2} = \frac{r^2}{m}\left(\frac{\partial^2 \psi}{\partial x^2} + \frac{\partial^2 \psi}{\partial y^2}\right) = 0$$

and (3) becomes $$\psi_M = \frac{1}{4}(\psi_A + \psi_B + \psi_C + \psi_D)$$

Fixing the value of ψ at one point on the outer boundary ($\psi = 0$ at B' in Fig.24), its value at the other points on this boundary is found from $\psi - 1/2\ r^2 =$ constant. As the inner boundary constant is at present unknowm, it is estimated at the ψ value on the outer boundary which lies on a mean circle, that is, it lies about the middle of the range of values on the outer boundary.

The relation which must be satisfied by ψ on any curve is

$$\int \frac{\partial \Psi}{\partial n} \cdot ds = 0 \qquad \text{(see 3.1).}$$

On a circle

$$\int \frac{\partial \Psi}{\partial n} \cdot ds = \int \frac{\partial \Psi}{\partial r} \cdot ds = \int \frac{\partial \psi}{\partial \xi} \cdot \frac{m}{r} \cdot r \cdot \frac{1}{m} \cdot d\eta$$

./

$\therefore \int \frac{\partial}{\partial} \frac{\psi}{\xi} \cdot d\eta = 0$ must hold on a ξ = constant line ..(12)

Again for a circle, solid or hollow,

$$\Psi = \text{const.} - \frac{1}{2} r^2 \quad \text{(see 3.1)}$$

and $\psi = \Psi + 1/2\, r^2 = $ const. over the section; thus ψ has a constant value on the section of the serrated shaft from $\xi = 0$ to $\xi = 8$ (found by trial); the effect of irregularity in the outer boundary does not extend into this region. The settling of the field from $\xi = 8$ to $\xi = 15.63$ solves the problem.

The value of ψ at $\xi = 8$ was quickly found, two estimations being sufficient, as shown, to satisfy (12) on this line.

The analytical method is particularly suitable for a problem of this type, since it makes full use of symmetry and regularity.

Finally, the stress factor $R = \partial\Psi/\partial n$. Here, as in most cases, the maximum stress occurs at a point on the boundary where the normal is a radial line.

At B' $$R = \frac{\partial \Psi}{\partial r} = \frac{m}{r} \cdot \frac{\partial}{\partial} \frac{\Psi}{\xi} - r$$

And $$C = 2A_1B_1 - 2A_2B_2 + 2\iint (\psi - \frac{1}{2} r^2)\, dx.dy$$

$$= 2A_1B_1 - 2A_2B_2 + \frac{2}{m^2}\iint (r^2\psi - \frac{1}{2} r^4)\, d\xi.d\eta$$

The/

The results are

$$C = 595; \qquad R = 13.3$$

When these are compared with a hollow circular shaft, 10" outside and 5.8" inside diameter, as standard, they give

Stiffness ratio, $C/C_s = 0.68$

Stress ratio, $R/R_s = 2.66$

Strength ratio $\dfrac{C/R}{C_s/R_s} = 0.256$ = ratio of torques,

producing the same maximum stress.
The strength ratio to that of a hollow shaft whose outer diameter equals the diameter at the bottom of the serrations is 0.414.

5. Bar of varying circular section.

Here equation (2) is to be solved on an axial section, rOz; the method is similar to that for solid bars (see 3.1). For estimating ψ values, consider sections where the diameter is constant or varying slightly, some distance from positions where it is changing rapidly such as OA, BC, Fig.25

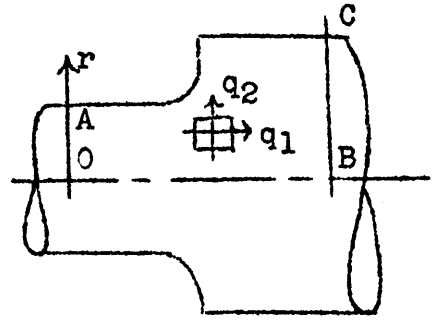

Fig. 25.

Here $\dfrac{\partial^2\psi}{\partial z^2} = 0$ and (2) becomes

$$\frac{\partial^2\psi}{\partial r^2} - \frac{3}{r}\cdot\frac{\partial\psi}{\partial r} = 0 \quad \text{giving } \psi = .kr^4$$

ψ /

ψ is then calculated for corners of squares on OA and BC, noting that since ψ is constant on the boundary, $\psi_A = \psi_C$. Also $\psi = 0$ on OB; therefore ψ is known completely on the boundaries of area OABC. Intermediate values are guessed to give regular increases.

When equation (3) is applied, we have

$$\psi_M = \frac{1}{4}(\psi_A + \psi_B + \psi_C + \psi_D) - \frac{3}{r} \cdot \frac{\partial \psi}{\partial r} \cdot \frac{s^2}{8}$$

Hence $\partial\psi/\partial r$ is to be found from the estimated values, and in the cases tried it was sufficient to take first differences. Thus for the point, E midway between C and B,

$$\frac{\partial \psi}{\partial r} = \frac{\psi_B - \psi_C}{S}$$

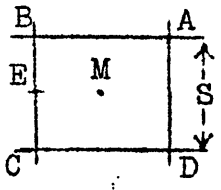

Also since this correction was small it did not change as the ψ values altered slightly on settling.

The stresses are, Fig. 25,

$$q_1 = \frac{N}{r^2} \cdot \frac{\partial \psi}{\partial r}, \quad q_2 = -\frac{N}{r^2} \cdot \frac{\partial \psi}{\partial z}$$

Hence the stress on the boundary, is given by

$$q = \frac{N}{r^2} \cdot \frac{\partial \psi}{\partial n} = \frac{N}{r^2}\sqrt{\left(\frac{\partial \psi}{\partial r}\right)^2 + \left(\frac{\partial \psi}{\partial z}\right)^2}$$

where n is the normal to the boundary. It is a maximum on the boundary.

For/

For the twist, let φ be the angular position of any point with reference to its unstrained position

$$\therefore q_1 = Nr \frac{\partial \varphi}{\partial z} = \frac{N}{r^2} \cdot \frac{\partial \psi}{\partial r} \qquad \therefore \frac{\partial \varphi}{\partial z} = \frac{1}{r^3} \cdot \frac{\partial \psi}{\partial r}$$

So the twist between two cross sections whose radii remain straight, such as OA, BC, Fig. 25, is found by integrating

$$\int_0^{OB} \frac{1}{r^3} \cdot \frac{\partial \psi}{\partial r} \cdot dz \qquad \text{along a line } r = \text{constant}$$

Two cases were considered.

1. Shaft enlarging to greater diameter.

Max. stress at P = 1.52 × stress on the smaller circle.

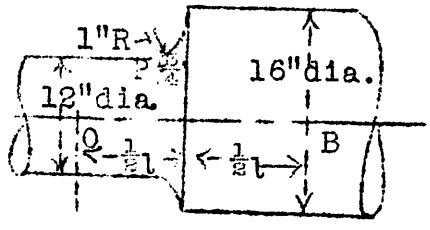

The twist may be found by taking an equivalent extra length 0.58" of the 12" diameter shaft, to allow for the junction. That is, for length OB = l, with the junction at its mid-point, the twist is the same as l/2 + 0.58" of 12", and l/2 of 16".

2. Shaft with collar. Max. stress at P = ~~1.50~~ 1.47 × stress on the shaft.

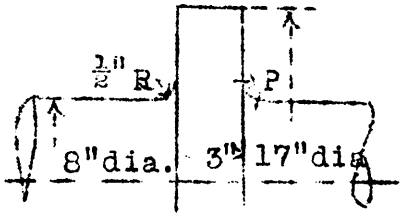

The twist is found, as for case 1, by taking an equivalent length of shaft = 1.06" to allow for the junctions. Or, length l including the collar has the same twist as l - 1.66" of shaft.

The/

The experimental work of this paper was carried out in the James Watt Engineering Laboratories, Glasgow University. I wish to acknowledge my indebtedness to Professor Cormack for helpful suggestions and encouragement, and also to Dr. Thom, whose method of analysis forms the basis of this paper, for his assistance in its application to this problem.

B.

THE SOLUTION OF THE TORSION PROBLEM FOR CIRCULAR SHAFTS OF VARYING RADIUS.

By Alexander Thom, D.Sc., Ph.D.

James Orr, B.Sc.

(Communicated by R.V.Southwell, F.R.S.

-- Received December 16th, 1930)

Introduction. When a bar of circular section whose radius is a function of z, fig.1, is subjected to terminal couples applied in a suitable way, the stresses and strains may be expressed* in terms of a function ψ . This function satisfies the equation

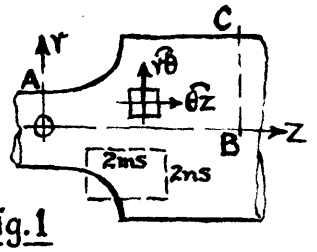

Fig.1

$$\frac{\partial^2\psi}{\partial r^2} - \frac{3}{r}\cdot\frac{\partial\psi}{\partial r} + \frac{\partial^2\psi}{\partial z^2} = 0 \quad \text{------(1)}$$

throughout an axial section, with ψ = constant on the boundary. The stresses are

$$\widehat{\theta z} = \frac{\mu}{r^2}\cdot\frac{\partial\psi}{\partial r} \quad , \quad \widehat{r\theta} = -\frac{\mu}{r^2}\cdot\frac{\partial\psi}{\partial z}$$

where μ is the modulus of rigidity of the material. The displacement, v, of any point is directed at right angles to an axial plane passing through the point, and is given by

$$r^3\cdot\frac{\partial}{\partial r}\left(\frac{v}{r}\right) = -\frac{\partial\psi}{\partial z} \quad , \quad r^3\cdot\frac{\partial}{\partial z}\left(\frac{v}{r}\right) = \frac{\partial\psi}{\partial r}$$

Equation (1) has been solved for certain boundaries by the usual analytical methods; for the general case ((including boundaries of non-mathematical form), the only method so far developed is an approximate graphical one due to Willers†. The present paper describes an arithmetical trial and error method, applicable to the general case, which may be carried to any desired degree of accuracy. An appendix to the paper mentions other physical problems which can be treated by similar methods.

Method of Solution. The boundaries are drawn to a suitable scale on squared paper, so that estimated ψ

---

*Love, "Mathematical Theory of Elasticity", 4th.edn,p.325

†Willers, "Z. Math. Phys.", vol.55 (1907)

values may be written at the corners of the squares. To find the corresponding values of ψ at the centres of the squares, we have, using Taylor's Theorem

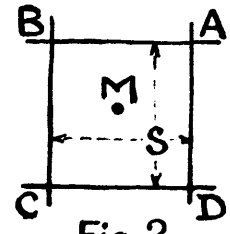

Fig.2

$$\psi_A = \psi_M + \tfrac{1}{2}s\cdot\frac{\partial\psi}{\partial r} + \tfrac{1}{2}s\frac{\partial\psi}{\partial z} + \tfrac{1}{8}s^2\cdot\frac{\partial^2\psi}{\partial r^2} + \tfrac{1}{4}s^2\frac{\partial^2\psi}{\partial r\,\partial z} + \tfrac{1}{8}s^2\frac{\partial^2\psi}{\partial z^2} - -$$

and similar expressions for ψ_B, ψ_C, ψ_D

$$\therefore\ \psi_M = \tfrac{1}{4}(\psi_A+\psi_B+\psi_C+\psi_D) - \tfrac{1}{8}s^2\nabla^2\psi - \tfrac{1}{384}s^4\left(\nabla^4\psi + 4\frac{\partial^4\psi}{\partial r^2\partial z^2}\right)-$$

Sub

Substituting from (1), $\nabla^2\psi = \frac{3}{r}\cdot\frac{\partial\psi}{\partial r}$, and neglecting the

the terms with 4th order and higher derivatives

$\psi_M = \frac{1}{4}(\psi_A+\psi_B+\psi_C+\psi_D) - \gamma$, where $\gamma = \frac{1}{8}s^2\cdot\frac{3}{r}\cdot\frac{\partial\psi}{\partial r}$ ----(3)

The term γ is obtained from the estimated ψ values; it is a small correction and in all cases which have been tried, it was sufficiently accurate to take

$$\frac{\partial\psi}{\partial r} \text{ at M (fig.2)} = \tfrac{1}{2}\cdot\frac{\psi_A-\psi_D}{s} + \tfrac{1}{2}\cdot\frac{\psi_B-\psi_C}{s}$$

Hence, an approximation to the values of ψ at the centres of the squares may be found, and used, by applying (3) again, to find a new approximation to the original corner values. This approximation is in general better than the assumed values (see below), that is, the process is convergent. Continuing, the process is repeated until the values cease changing, when equation (1) is satisfied to the approximation of (3). An actual example of the method is given later in the paper.

We have still to examine whether the neglected terms in (2) are in fact negligible. This is easily tested at any part of the section, when the values have settled, by enlarging that part, using smaller squares and finding if the values alter, for the neglected terms diminish in importance with the size of the square. Now

the higher derivatives are, in general, greatest near portions of the boundary which change direction quickly, so it is necessary in many cases to enlarge the section near these parts

In estimating the preliminary ψ values, consider the regions where the boundary radius is constant, or varies slightly with z, such as OA, OB, fig.1, some distance from positions where it is changing rapidly. For these regions $\frac{\partial^2\psi}{\partial z^2} = 0$, and (1) becomes

$$\frac{\partial^2\psi}{\partial r^2} - \frac{3}{r}\cdot\frac{\partial\psi}{\partial r} = 0, \qquad \text{giving } \psi = kr^4$$

The value of ψ is then calculated for corners of squares on OA and BC, noting that since is constant on the boundary $\psi_A = \psi_C$ Also $\psi = 0$ on OB; Therefore it is known completely on the boundary OABC. Intermediate values are guessed to give regular increases.

Where a boundary does not pass through the corner of a square, the adjacent ψ value must be found by interpolation. For about 1% accuracy this may be done graphically, but greater accuracy requires numerical interpolation.

Convergence. This will be considered in two steps, (a) when the term γ in (3) is small and therefore changes in it are negligible, as in all examples yet solved by this method; and (b) when changes in it are not negligible.

(a). Let the size of the square be such that neglected terms in (2) do not affect the last significant figure at any part of the section. Let ε denote the error in the assumed value of ψ ; the estimated values are then $\psi + \varepsilon$. Including ε in (3) we have

$$\psi_M + \varepsilon_M = \tfrac{1}{4}\Sigma\psi + \tfrac{1}{4}\Sigma\varepsilon - \gamma$$

since $\psi_M = \tfrac{1}{4}\Sigma\psi - \gamma$

subtracting $\varepsilon_M = \tfrac{1}{4}\Sigma\varepsilon - \tfrac{1}{4}\Sigma\psi$ - - - - - - (4)

$\tfrac{1}{4}\Sigma\varepsilon$

where Σ denotes the sum of the corner values. ε_m is the error in the approximation to the centre value on applying (3).

Let fig.3 give the variation of ψ and ε along a line, z = const. Assume for convenience of representation that ε does not vary with z. The successive approximations are shown in the lower figure, which gives ε alone, and it is seen that abrupt changes in it are smoothed out, while it creeps steadily to zero. In this diagram, abcd is the error surface which alters, on applying (3) twice, to efgd.

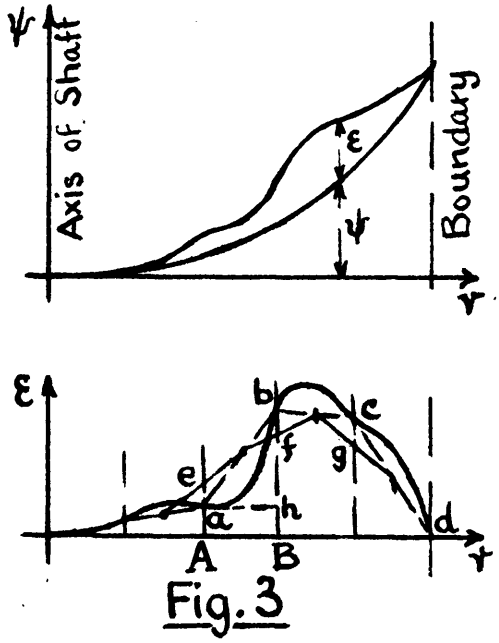

Fig.3

This point is also illustrated by finding a relation between ε and δ, where δ is the difference obtained in the estimated ψ value by applying (3) twice, first to obtain the central values and again from these, to obtain new corner values (a double round). If ε is the error at a corner, its value at the surrounding corners may be expressed by Taylor's Theorem, in terms of its first and second derivatives as shown at the nine main corners in fig.4.

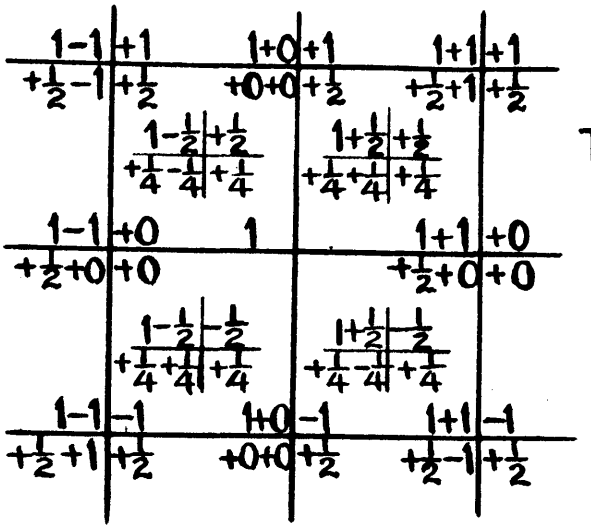

The numbers are coefficients of

$$\varepsilon,\ s\frac{\partial\varepsilon}{\partial z},\ s\frac{\partial\varepsilon}{\partial r}\ \Big|\ s^2\frac{\partial^2\varepsilon}{\partial z^2},\ s^2\frac{\partial^2\varepsilon}{\partial r\partial z},\ s^2\frac{\partial^2\varepsilon}{\partial r^2}$$

Fig.4

The four centre values are then found from (4). Another application of (4) gives the new central error, which is then found to exceed the original by

$$\delta = \tfrac{1}{4}s^2.\nabla^2\varepsilon \qquad \text{- - - - - - (5)}$$

When the error surface is concave up, $\nabla^2\varepsilon$ and so δ are positive, that is, hollows fillup; similarly, peaks flatten. This formula shows that the first tendency is to smooth out abrupt changes in ε, for in these regions $\nabla^2\varepsilon$ has a high value, and the second tendency is to diminish ε gradually over the section.

(b). When the changes in γ are not negligible, (4) becomes $\varepsilon_M = \tfrac{1}{4}\Sigma\varepsilon - \tfrac{1}{8}s^2.\frac{3}{r}.\frac{\partial\varepsilon}{\partial r}$.

It will be shown that the effect of the second term is to hasten the convergence. Referring to fig.3, the typical variation of the error along a line, z = const., is shown; it is zero for some distance near the r = 0 end, since ψ there is small, and also irregularities in the boundary scarcely affect this region.

Consider the square, two of whose corners are A and B, fig.3; here $s.\frac{\partial\varepsilon}{\partial r}$ is hb, giving $\frac{1}{8}.s^2.\frac{3}{r}.\frac{\partial\varepsilon}{\partial r} = \frac{3}{8}.\frac{s}{r}.(hb)$ Since $\frac{s}{r} < 1$ except for the first square, the effect of

this term is never violent, and it decreases as r increases; it hastens the convergence where $\frac{\partial \varepsilon}{\partial r}$ and ε have the same sign, which occurs in general at the smaller values of r; it retards the convergence where they have different signs, which occurs in general at the higher values of r. Now, this term is less important at the higher values of r, the region where the convergence is retarded, hence, the general effect is to hasten the convergence.

Shortening the Process. If an approximate average value of the ratio $\frac{\varepsilon}{\delta}$ could be estimated for a part of the section, the slow creep of the successive approximations could be quickened. Consider a rectangular part of the section including $2m \times 2n$ squares of side s, fig.1; assume that ψ is known on the sides so that the error there is zero. Let the error take the simple form

$$\varepsilon = \varepsilon_0 \left(1 - \frac{r^2}{n^2 s^2}\right)\left(1 - \frac{z^2}{m^2 s^2}\right)$$

where ε_0 is the error at the centre of the rectangle, the origin of coordinates. From (5)

$$\delta = \tfrac{1}{4} s^2 . \nabla^2 \varepsilon = -\tfrac{1}{2} \varepsilon_0 \left(\frac{1}{m^2} + \frac{1}{n^2} - \frac{r^2 + z^2}{m^2 n^2 s^2}\right)$$

$$\therefore \frac{\varepsilon_0}{\delta_0} = -\frac{2}{\left(\frac{1}{m^2} + \frac{1}{n^2}\right)}$$

and the average value of ε/δ is less than this. It is found that using

$$\varepsilon/\delta = -1.5 \Big/ \left(\frac{1}{m^2} + \frac{1}{n^2}\right) \text{ ------ (6)}$$

over the part of the section considered gives good results in practice. The best procedure is to take two double rounds, and apply (6) to the differences obtained by the second.

In actual cases, equivalent values of m and n are estimated; for example, in the case of a shaft enlarging to greater diameter, fig.1, the equivalent rectangle is usually as shown, enclosing the region of great error. This method gives better results than might appear at

first sight, for, with the differences δ all over the section, obtained by applying a double round, the operator can tell, after a little experience, where the error is great and where it is nearly zero. Further, if the multiplier (6) is incorrectly estimated, its general effect can be observed when the next double round is taken, and so may be altered to suit.

Example. To illustrate the method, the example of a shaft with collar is given in full, figs. 5 and 6.

First, the values are estimated; on the line $z = -1$, $\psi = kr^4$, so , taking any convenient number (in the example 41), as the boundary value, intermediate values are guessed to give regular increases.

The term γ is calculated throughout the section from the estimated values, and is shown by numbers enclosed in circles in fig.5.

Now the correcting process can proceed. By applying (3), the values are found at the centres of the squares, a comptometer proving very useful for this step; applying (3) again to the centre values a better approximation to the corner values is obtained. The differences between the second and first approximations are written down so that a double round may be repeated on them, the smaller numbers making this easier than the first round..

As the formula for shortening the process is applied at this stage, a rectangle is sketched in, which surrounds the region requiring much correction. In the example the rectangle is bounded by the lines $z = 3$, $z = 9$, $r = 6$, $r = 11$. From (6) $\varepsilon/\delta = -1.5 / (1/9 + 1/6.2) = -6$ Hence the differences from the last double round are

SHAFT WITH COLLAR

SOLUTION OF $\nabla^2\psi = \frac{2}{r}\cdot\frac{\partial\psi}{\partial r}$

$\frac{s^2}{8}\cdot\frac{3}{r}\cdot\frac{\partial\psi}{\partial r}$ shown ⑥

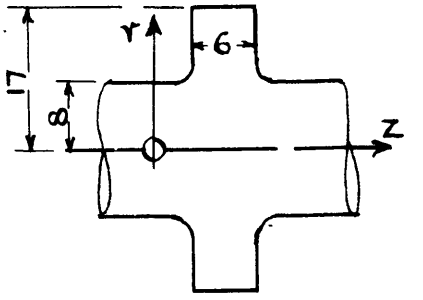

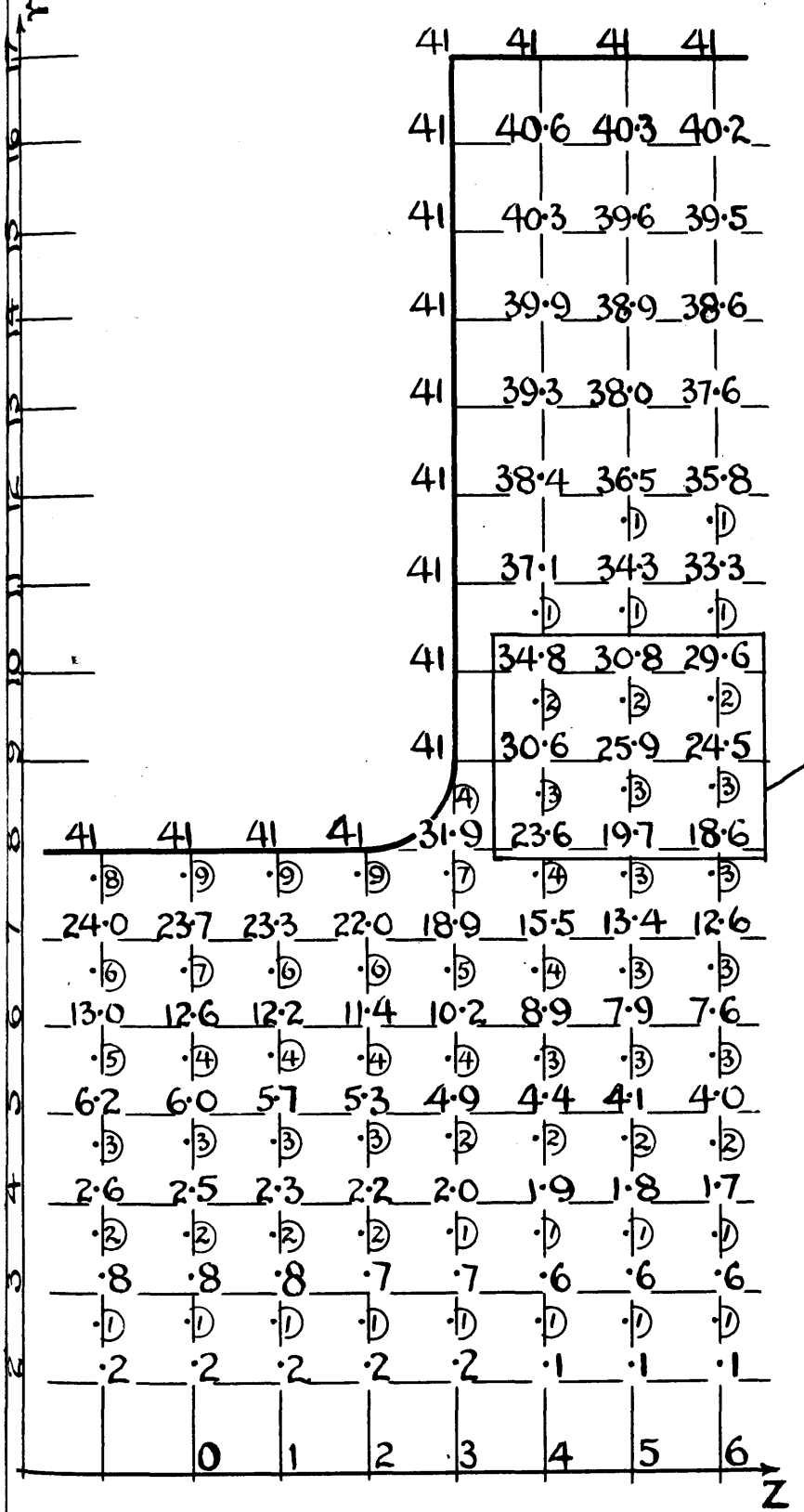

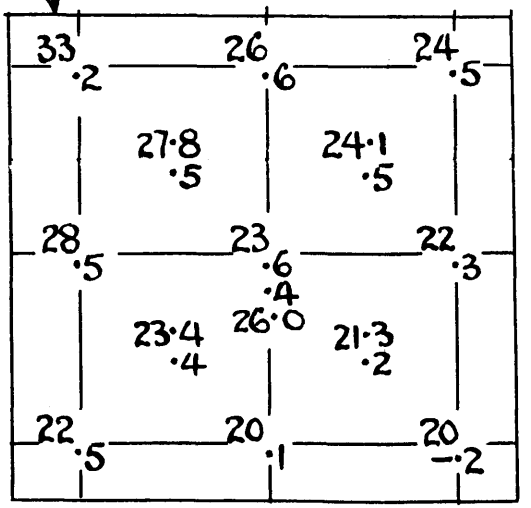

(a)

This shows the effect on ψ at the point $(r=9, z=5)$, of two double rounds and formula (6) starting from preliminary estimated values

FIG. 5

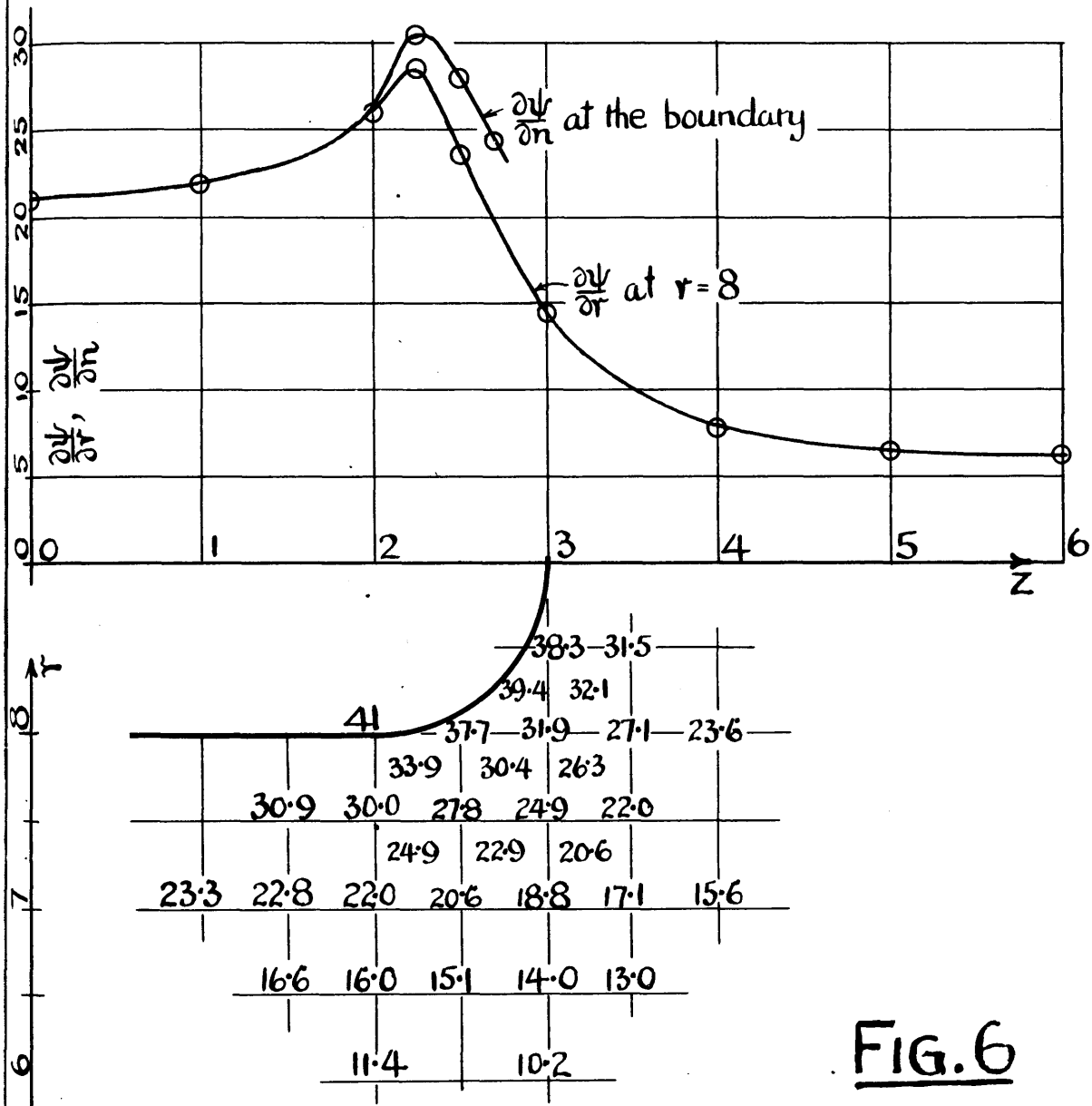

FIG. 6

ENLARGEMENT AT JUNCTION

Outer values are deduced from squares thus ◇

Inner values (close to the junction between shaft and collar) are deduced from squares thus □

multiplied by 6 to obtain the next approximation. The application to a few values is shown at (a), fig.5; for the centre point $\psi + \epsilon_1 = 23$, the first double round gives $\delta_1 = 0.6$, the second gives $\delta_2 = 0.4$, therefore the second approximation is

$\psi + \epsilon_2 = 23 + 0.6 + 6 \times 0.4 = 26.0$ The value at this point when the field has finally settled is 25.9.

Having settled the values on the section with this size of square, we next investigate the effect of the neglected terms in (2) by reducing the size of square to half at various parts, and finding if the values alter. In this case it is found that they alter only near the junction of shaft and collar, and this region is shown enlarged in fig.6.

When the values cease changing, the problem is solved, and the final step of finding the stresses and strains may be taken. The maximum stress occurs on the boundary; it is equal to $\sqrt{\{(\bar{\theta z})^2 + (\bar{r\theta})^2\}} = \frac{\mu}{r^2}\sqrt{\{(\frac{\partial \psi}{\partial r})^2 + (\frac{\partial \psi}{\partial z})^2\}} = \frac{\mu}{r^2} \cdot \frac{\partial \psi}{\partial n}$

where dn is the normal to the boundary. The simplest and most accurate method of finding these derivatives, is to use difference formulae. The stress on the boundary, from z = 0 to z = 2.7, is plotted in fig.6; the maximum stress occurs at z = 2.25, and = 1.47 × stress on the boundary at z = 0.

The angular position, (v/r), of any point with reference to its unstrained position, is given by

$$\frac{\partial}{\partial z}\left(\frac{v}{r}\right) = \frac{1}{r^3} \cdot \frac{\partial \psi}{\partial r}$$

So the twist of the cross section at z = 12, relatively to the section at z = 0, is found by integrating $\frac{1}{r^3} \cdot \int_0^{12} \frac{\partial \psi}{\partial r} \cdot dz$ along a line, r = const. Here $\frac{\partial \psi}{\partial r}$ is found along r = 8 and is shown plotted in fig.6. The twist on this 12" length is the same as that for a

length of 8.7" of an 8" radius shaft, subjected to the same torque.

The methods discussed in this paper have been developed in connection with experimental work, which is being carried out in the James Watt Engineering Laboratories, University of Glasgow, under the directorship of Professor J.D.Cormack.

Appendix. Similar methods have been applied to the solution of other physical problems, namely -

(a) Torsion of prisms with non-circular sections; the equation to be solved is $\frac{\partial^2\Psi}{\partial x^2} + \frac{\partial^2\Psi}{\partial y^2} + 2 = 0$ with Ψ = const. on each boundary. Actual cases for which a solution has been obtained include a shaft with keyway, several British Standard structural sections, a hollow square and a hollow serrated shaft. In several of these cases, tests on specimens gave experimental verification.

(b) * Perfect fluid flow in two dimensions; the equation is $\frac{\partial^2\psi}{\partial x^2} + \frac{\partial^2\psi}{\partial y^2} = 0$, with ψ = const. on a fixed boundary.

(c) Viscous fluid flow in two dimensions; the equations to be solved are

$$\nu.\nabla^2\zeta = -\frac{\partial\psi}{\partial y}.\frac{\partial\zeta}{\partial x} + \frac{\partial\psi}{\partial x}.\frac{\partial\zeta}{\partial y}$$

$$\nabla^2\psi = 2\zeta$$

A solution* has been obtained for the flow past a cylinder at Reynold's Number = 10, which was consistent with experimental results.

The solution in cases (a) and (b) is straightforward and the remarks on convergence given above, apply to these case also. In case (c) it is necessary to solve two fields simultaneously, one for the stream function(Ψ), the other for the vorticity (ζ). A consideration of the flow between parallel plates indicated that the process may not be convergent if the size of the square exceeds some limiting figure.

*Thom, Aer.Res.Com. R & M, 1194.